

A 3D visualization of a catalytic surface, likely a metal nanoparticle or cluster, rendered in a vibrant rainbow color gradient from purple to yellow. The surface is highly textured and porous. A molecular model, possibly representing a reactant or product, is shown interacting with the surface. The background is dark, making the colorful surface stand out.

**BORESKOV INSTITUTE  
OF CATALYSIS**

**PHYSICOCHEMICAL  
METHODS OF RESEARCH**

## Preface



The Boreskov Institute of Catalysis is a unique team of highly qualified specialists successfully addressing challenges in the field of catalysis, from fundamental problems to catalyst design and development of industrial catalytic processes. Fundamental scientific studies performed by BIC team are the basis of many existing catalytic technologies implemented at largest companies in Russia and other countries. Many applied investigations are carried out within the framework of the most important federal programs and aimed to maintain the economic stability of Russia.

Scientific research at the highest world level certainly implies the availability of advanced state-of-the-art technologies. Indeed, the level of fundamental and applied studies in a chemical research institute is largely determined by the physicochemical methods at its disposal. That is why BIC pays a particular attention to the development and application of sophisticated physicochemical methods at the atomic and molecular level. The Boreskov Institute of Catalysis is one of the best equipped chemical institutions in Russia and possesses a unique complex of the most advanced equipment that allows our highly qualified specialists to obtain the world-level results in the field of catalysis. Some of these results can be found in numerous high-ranking publications in the top-level peer reviewed journals.

One of the highest priority of Boreskov Institute of Catalysis is the development of physicochemical methods for *in situ* studies of catalyst properties and mechanism of catalytic reactions. To investigate an actual catalytic process, to look at the catalyst at work in real time used to be a long-held dream of many generations of scientists, which comes true today. The knowledge and exceptional information obtained via one-of-a-kind equipment is a powerful tool for the research and development of catalysts and catalytic processes.

The unparalleled equipment and physicochemical methods available at Boreskov Institute of Catalysis are used in the major joint multidisciplinary projects that consolidate the experts in various fields of science and technology. BIC participates in a number of large international and national projects and collaborates with numerous manufacturers of catalysts, factories, plants in Russia and abroad. Boreskov Institute of Catalysis has a rich and long-term experience of close cooperation with many international majors working in the field of chemistry, petrochemistry, oil and gas processing, etc. Suffice it to say that the Institute is involved in different forms of international collaboration with 8 out of 10 top ICIS chemical companies worldwide. Boreskov Institute of Catalysis is always open for the cooperation and ready for the global challenges of present-day high-tech world!

Prof. Oleg N. Martyanov  
Vice-director  
Head of Physicochemical Methods Department, Boreskov Institute of Catalysis

# Table of Contents

<b>X-Ray Diffraction and Scattering.....</b>	<b>04</b>
X-Ray Powder Diffraction (XRD).....	04
<i>In Situ</i> X-Ray Diffraction.....	06
X-Ray Diffraction Research Complex on Synchrotron Radiation.....	08
X-Ray Absorption Spectroscopy: Extended X-Ray Absorption Fine Structure (EXAFS)	
X-Ray Absorption Near Edge Structure (XANES).....	12
Small Angle X-Ray Scattering (SAXS).....	14
<b>Microscopy.....</b>	<b>16</b>
Scanning Electron Microscopy (SEM).....	16
Scanning Tunneling Microscopy (STM).....	20
Transmission Electron Microscopy (TEM).....	22
<b>Surface Science.....</b>	<b>26</b>
X-Ray Photoelectron Spectroscopy (XPS), Electron Spectroscopy for Chemical Analysis (ESCA).....	26
High Pressure X-Ray Photoelectron Spectroscopy (HP XPS).....	28
Polarization Modulation InfraRed Reflection Absorbption Spectroscopy (PM IRRAS).....	30
<b>Magnetic Resonance.....</b>	<b>32</b>
Nuclear Magnetic Resonance (NMR) Spectroscopy.....	32
<i>In Situ</i> Magic Angle Spinning Nuclear Magnetic Resonance (MAS NMR) Spectroscopy.....	36
Electron Spin Resonance (ESR) Spectroscopy.....	44

<b>Fourier-Transformed Infrared Spectroscopy (FT-IR)</b> .....	48
Fourier-Transformed Infrared Spectroscopy (FT-IR).....	48
Fourier-Transformed Infrared Spectroscopy in Supercritical Fluids (SCF) <i>In Situ</i> .....	50
Wide Temperature FT-IR Spectroscopy of Adsorbed Molecules Using Transmission, Diffusion Reflection, and Attenuated Total Reflection (ATR) Technique.....	52
<b>Raman Spectroscopy</b> .....	54
<b>Ultraviolet-Visible (UV-Vis) Spectroscopy</b> .....	56
Ultraviolet-Visible Diffuse Reflectance Spectroscopy (UV-Vis DRS).....	56
Photoluminescence Spectroscopy.....	60
<b>Elemental Analysis</b> .....	62
X-Ray Fluorescence (XRF).....	62
Inductive-Coupled Plasma Mass-Spectrometry (ICP-MS).....	64
Inductively Coupled Plasma Optical Emission Spectroscopy (ICP-OES).....	66
<b>Chromatography</b> .....	68
<b>Textural Methods of Investigation</b> .....	74
<b>Steady-State Isotopic Transient Kinetic Analysis (SSITKA)</b> .....	80
<b>Calorimetry</b> .....	82

# X-Ray Diffraction and Scattering

## X-Ray Powder Diffraction (XRD)

### Scientific and analytical tasks

- Study of the phase composition of a wide range of polycrystalline materials and catalysts
- Determination and refinement of unit cell parameters
- Determination of coherent scattering domain values and microstrains
- Full-profile quantitative phase analysis of polycrystalline materials
- Refinement of the atomic structure parameters using a Rietveld method
- Determination of the degree of crystallinity using an internal standard method
- Development and application of methods for a structural analysis of disordered materials and nanocrystals

### Equipment

#### X-ray Powder Diffractometer Bruker D8

- $\text{CuK}\alpha_{1,2}$  (1.5418 Å) radiation source
- Linear positive-sensitive detector LynxEye (simultaneous measurement of intensity in the range  $2\theta = 2.9^\circ$  using 192 detector channels)
- Fluorescence and air-scattering filtration
- Bragg-Brentano geometry, the maximum angle interval  $5^\circ < 2\theta < 140^\circ$
- Configuration:  $\Theta$ - $\Theta$ , horizontal sample alignment
- Accuracy of the reflection position  $\pm 0.01^\circ$   $2\theta$  for a standard configuration if the sample position corresponds to the focal plane
- Tube operation mode: 35 kV, 35 mA
- Sample holders: single-crystal silicon cuvette, plastic cuvettes with various pocket diameters, dome-type sample holder for the samples unstable in ambient atmosphere
- The various standard plastic cuvettes allow XRD measurements for well-ground powders with a mean particle size 50 - 100  $\mu\text{m}$ . Sample volume 0.2 - 0.5  $\text{cm}^3$ . Samples should be stable under ambient conditions at least for 2 hours
- ICDD PDF-2 database of organic and inorganic compounds is used for a qualitative phase analysis
- TOPAS 4.3 (Bruker) program suite is used for a full-profile analysis

X-ray Powder

Diffractometer Bruker D8

## References

1. Coherent 3D nanostructure of  $\gamma$ -Al<sub>2</sub>O<sub>3</sub>; Simulation of whole X-ray powder diffraction pattern.  
*J. Solid State Chem.* **246** (2017) 284
2. Structure and morphology evolution of silica-modified pseudoboehmite aerogels during heat treatment.  
*J. Solid State Chem.* **233** (2016) 294
3. Debye function analysis of nanocrystalline gallium oxide  $\gamma$ -Ga<sub>2</sub>O<sub>3</sub>.  
*Z. Kristallographie* **231** (2016) 261
4. Ceramic matrix composites prepared from CoAl powders.  
*J. Materials Sci.* **51** (2016) 10487
5. Synthesis of Pt/Zn(OH)<sub>2</sub>/Cd<sub>0.3</sub>Zn<sub>0.7</sub>S for the photocatalytic hydrogen evolution from aqueous solutions of organic and inorganic electron donors under visible light.  
*Top. Catal.* **15-16** (2016) 1297
6. Thermal evolution of Mg-Al and Ni-Al layered double hydroxides: The structure of the dehydrated phase.  
*Acta Crystallogr., Sect. A: Found. Crystallogr.* **72** (2016) 651
7. Observation of the superstructural diffraction peak in the nitrogen doped carbon nanotubes: Simulation of the structure.  
*Fullerenes Nanotubes and Carbon Nanostructures* **24** (2016) 520
8. Effect of nitric oxide on the formation of cobalt-aluminum oxide structure from layered double hydroxide and its further transformation during reductive activation.  
*Appl. Catal. A* **514** (2016) 114
9. Preparation of porous ceramometal composites through the stages of mechanical activation and hydrothermal partial oxidation of Me-Al powders.  
*Catal. Today* **246** (2016) 232
10. Metal-support interaction in Pd/CeO<sub>2</sub> model catalysts for CO oxidation: From pulsed laser-ablated nanoparticles to highly active state of the catalyst.  
*Catalysis Science and Technology* **6** (2016) 6650
11. Effect of K and Bi doping on the M1 phase in MoVTenbO catalysts for ethane oxidative conversion to ethylene.  
*Appl. Catal. A* **514** (2016) 1
12. Nano-domain states of strontium ferrites SrFe<sub>1-y</sub>MyO<sub>2.5-x</sub> (M=V, Mo; Y ≤ x ≤ 0.2).  
*J. Solid State Chem.* **225** (2015) 410
13. Structure of oxides prepared by decomposition of layered double Mg-Al and Ni-Al hydroxides.  
*J. Solid State Chem.* **225** (2015) 417
14. On the effect of Cu on the activity of carbon supported Ni nanoparticles for hydrogen electrode reactions in alkaline medium.  
*Top. Catal.* **58** (2015) 1181
15. Direct CO<sub>2</sub> capture from ambient air using K<sub>2</sub>CO<sub>3</sub>/Y<sub>2</sub>O<sub>3</sub> composite sorbent.  
*Fuel* **127** (2014) 212
16. The local structure of Pd<sub>x</sub>Ce<sub>1-x</sub>O<sub>2-x/2</sub> solid solutions.  
*PCCP* **16** (2014) 13523



# X-Ray Diffraction and Scattering

## In Situ X-Ray Diffraction

### Scientific and analytical tasks

- Development and application of *in situ* X-ray diffraction for the study of physical and chemical processes in various atmospheres and temperatures
- The study of phase composition, structural (unit cell parameters, crystal structure) and microstructural characteristics of catalysts and functional materials during *in situ* measurement

### Equipment

#### Diffractometer Bruker D8 Advanced equipped with reactor chamber

#### Anton Paar XRK 900 or high-temperature strip heater chamber Anton Paar HTK 16N

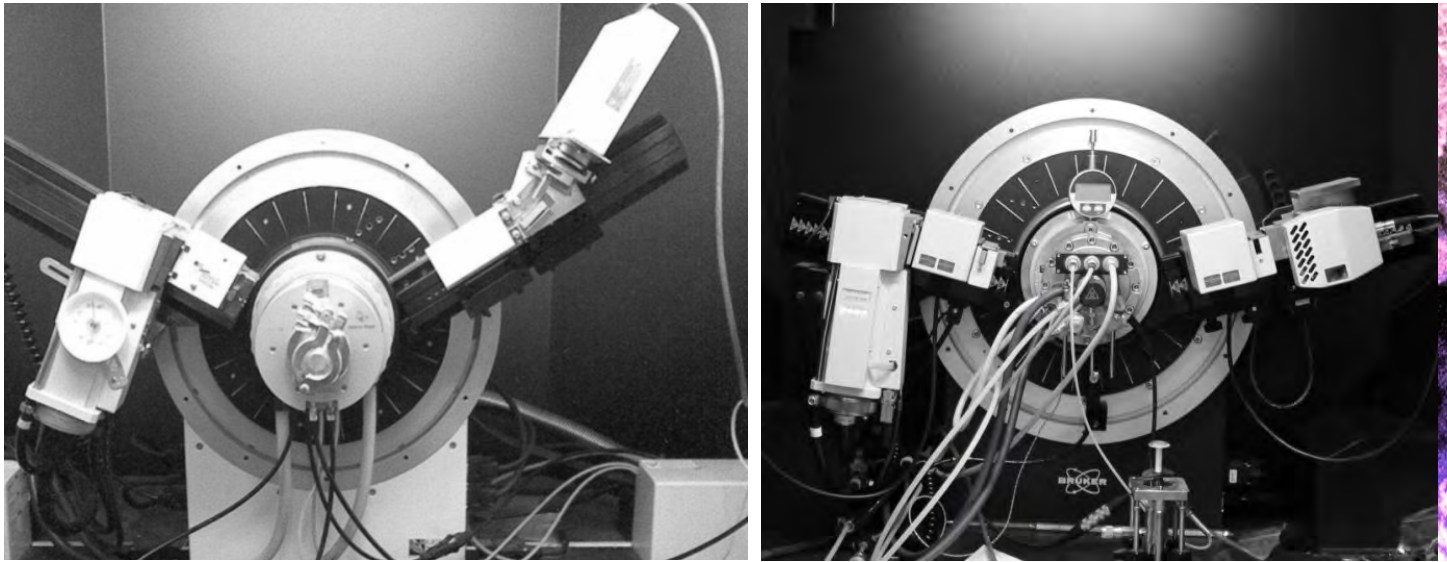
- Radiation: CuK $\alpha$  (40 kV, 40 mA)
- Detector: linear Lynxeye
- Geometry: focusing Bragg-Brentano and parallel-beam geometry with Göbel Mirror
- Configuration:  $\Theta$ - $\Theta$
- Accuracy of alignment: 0.002°
- Shooting mode: Single-step or continuous
- Tube mode: 40 kV, 40  $\mu$ a

#### Reactor Chamber: Anton Paar XRK 900

- Operating temperature: 25 °C to 900 °C
- Atmospheres: vacuum (1mbar), air, inert gas, reactive gas
- Max. housing temperature: 150 °C
- Angle of incidence: 0 to + 165° 2 $\Theta$
- Max. operating pressure: 1 mbar to 10 bar

## High-Temperature Strip Heater Chamber Anton Paar HTK 16N

- Operating temperature (vacuum, air, inert gas): 25 °C to 1600 °C
- Nitrogen: 1400 °C
- Helium: 1300 °C
- Atmospheres: vacuum ( $10^{-4}$  mbar), air, inert gas
- Max. operating pressure: 0.5 bar above atmospheric pressure
- Angle of incidence: 4 to  $164^\circ 2\theta$



## References

1. Low-and high-temperature oxidation of  $Mn_{1.5}Al_{1.5}O_4$  in relation to decomposition mechanism and microstructure. *Cryst. Eng Comm.* **18** (2016) 3411
2. New ferroelastic  $K_2Sr(MoO_4)_2$ : Synthesis, phase transitions, crystal and domain structures, ionic conductivity. *J. Solid State Chem.* **237** (2016) 64
3. Effect of heat treatment conditions on the structure and catalytic properties of  $MnO_x/Al_2O_3$  in the reaction of CO oxidation. *Appl. Catal., A* **459** (2013) 73
4. Direct  $CO_2$  capture from ambient air using  $K_2CO_3/Al_2O_3$  composite sorbent. *Int. J. Greenhouse Gas Control.* **17** (2013) 332
5. *In situ* XRD, XPS, TEM and TPR study of highly active in CO oxidation CuO nanopowders. *The Journal of Physical Chemistry C* **117** (2013) 14588
6. Cobalt borate catalysts for hydrogen production via hydrolysis of sodium borohydride. *J. Alloys Compd.* **513** (2012) 266
7. High-temperature X-ray study of the formation and delamination of manganese-alumina spinel  $Mn_{1.5}Al_{1.5}O_4$ . *J. Struct. Chem.* **50** (2009) 474

# X-Ray Diffraction and Scattering

## X-Ray Diffraction Research Complex on Synchrotron Radiation

### Scientific and analytical tasks

- Determination and refinement of phase composition, structure and microstructure parameters of polycrystalline functional materials
- *In situ* studies of structure transformation of functional materials under high temperature and reaction media

### Equipment

The Research Complex comprises two experimental stations mounted on No.2 and No.6 SR Beamlines of VEPP-3 electron storage ring at Siberian Synchrotron and Terahertz Radiation Center, Budker Institute of Nuclear Physics SB RAS.

- **The station at No.2 Beamline** is designed for high precision studies of the structure of functional materials under normal condition

### Station parameters:

- Working photon energy range  $5 \div 20$  keV
  - Energy resolution of monochromator  $E/E \sim (1 \div 5) \cdot 10^{-4}$ ; ability to use resonant effects for structure investigation
  - High instrumental resolution  $d/d \sim 5 \cdot 10^{-5}$  at photon energy  $\sim 10$  keV
  - Exposure time for X-ray diffraction pattern  $0.1 \div 6$  hours depending on angular range, scan step and point exposure
- **The station at No.6 Beamline** is designed for studies of structure and structure transformation of functional materials under high temperature and reaction media with time-resolved experiments

### The station is equipped with:

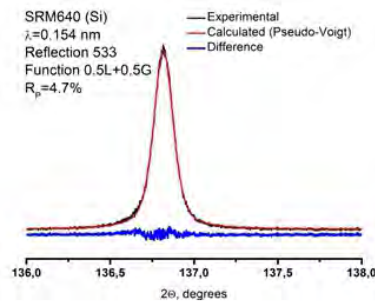
- X-ray one-coordinate position sensitive detector OD-3M-350
- High temperature X-ray diffraction chamber Anton Paar HTK-2000
- X-ray diffraction reactor chamber Anton Paar XRK-900
- Flow-mass controllers Sierra SmartTrack 50
- Gas mixture pressure gauge
- Mass spectrometer SRS UGA100
- Hydrogen generator

## The station parameters:

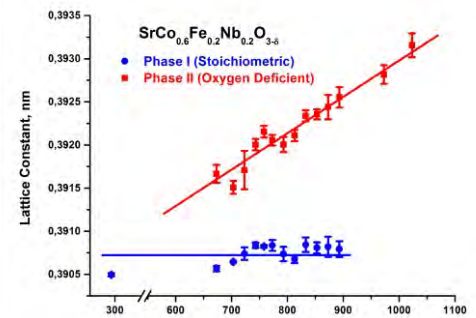
- Single-fold reflection monochromator with Ge(111), Si(111), Si(220), Si(311) crystals
- Working photon energies 7.16, 7.46, 12.2 and 14.6 keV, respectively
- Monochromator energy resolution  $E/E \sim (2 \div 5) \cdot 10^{-4}$
- Registration of X-ray diffraction patterns simultaneously over angular range of  $\sim 30^\circ$  with resolution of  $\sim 0.01^\circ$  and time resolution of several microseconds up to several minutes
- Temperature range of high temperature X-ray diffraction chamber Anton Paar HTK-2000 from RT up to 1400 °C in air and up to 2000 °C in vacuum
- Pressure range within chamber from  $10^{-7}$  mbar to 1 bar
- Temperature range of X-ray diffraction reactor chamber Anton Paar XRK-900 from RT up to 750 °C in hydrogen or helium and up to 900 °C in reaction mixture
- Gas mixture pressure range within reactor chamber from 1 mbar up to 10 bar



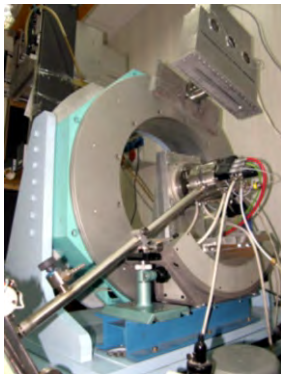
Experimental station at No.2 SR Beamline



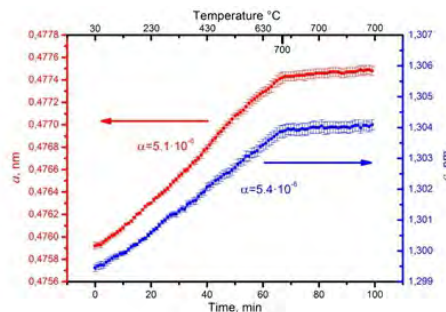
Peak shape of SRM640 (Si) reflection (533)



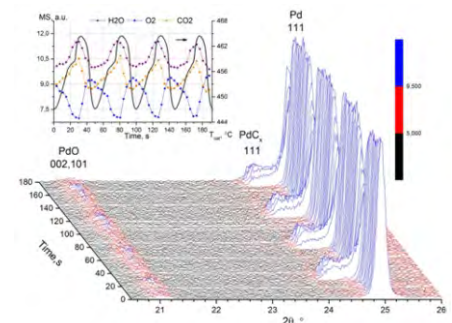
High resolution XRD study of variation of lattice constant and phase composition of  $\text{SrCo}_{0.6}\text{Fe}_{0.2}\text{Nb}_{0.2}\text{O}_{3-\delta}$  oxygen conductor with temperature of calcination in vacuum



Experimental station at No.6 SR Beamline



Thermal expansion of corundum while heated in inert atmosphere



Self-sustained kinetic oscillations in the catalytic oxidation of methane over Pd

## References

1. Effect of nitric oxide on the formation of cobalt-aluminum oxide structure from layered double hydroxide and its further transformation during reductive activation.  
*Appl. Catal., A* **514** (2016) 114
2. Comparison of growth mechanisms of undoped and nitrogen-doped carbon nanofibers on nickel-containing catalysts.  
*Cuihua Xuebao / Chinese Journal of Catalysis* **37** (2016) 169
3. Thermal expansion of iron carbides, Fe<sub>3</sub>C<sub>2</sub> and Fe<sub>3</sub>C, at 297-911 K determined by *in situ* X-ray diffraction.  
*J. Alloys Compd.* **628** (2015) 102
4. User-friendly synthesis of highly selective and recyclable mesoporous titanium-silicate catalysts for the clean production of substituted p-benzoquinones.  
*Catal. Sci. & Technol.* **4** (2014) 200
5. Highly selective H<sub>2</sub>O<sub>2</sub>-based oxidation of alkylphenols to p-benzoquinones over MIL-125 metal-organic frameworks.  
*Eur. J. Inorg. Chem.* **2014** (2014) 132
6. Ammonia sorption on the composites "(BaCl<sub>2</sub> + BaBr<sub>2</sub>) inside vermiculite pores".  
*Colloids Surf., A* **448** (2014) 169
7. *In situ* X-ray diffraction studies of Pr<sub>2-x</sub>NiO<sub>4-x</sub> crystal structure relaxation caused by oxygen loss.  
*Solid State Ionics* **262** (2014) 918
8. *In situ* X-ray diffraction study of the growth of nitrogen-doped carbon nanofibers by the decomposition of ethylene-ammonia mixture on a Ni-Cu catalyst.  
*Carbon* **52** (2013) 486
9. A correlation between structural changes in a Ni-Cu catalyst during decomposition of ethylene/ammonia mixture and properties of nitrogen-doped carbon nanofibers.  
*J. Energy Chem.* **22** (2013) 270
10. *In situ* and *ex situ* time resolved study of multi-component Fe-Co oxide catalyst activation during MWNT synthesis.  
*Physica Status Solidi (B)* **249** (2012) 2390
11. Superhard nanocrystalline Ti-Cu-N coatings deposited by vacuum arc evaporation of a sintered cathode.  
*Surf. Coat. Technol.* **207** (2012) 430
12. *In situ* study on changes in the phase composition of a Ni-Cu catalyst during growth of nitrogen-containing carbon nanofibers.  
*Published in Doklady Akademii Nauk*, 2011, Vol. 439, No. 1, pp. 72-75
13. Structural changes in a nickel-copper catalyst during growth of nitrogen-containing carbon nanofibers by ethylene/ammonia decomposition.  
*Carbon* **48** (2010) 2792
14. Mesoporous "core-shell" adsorbents and catalysts with controllable morphology.  
*Appl. Surf. Sci.* **256** (2010) 5513
15. Magnetically separable titanium-silicate mesoporous materials with core-shell morphology: Synthesis, characterization and catalytic properties.  
*J. Mater. Chem.* **19** (2009) 7332
16. Heterogeneous selective oxidation catalysts based on coordination polymer MIL-101 and transition metal-substituted polyoxometalates.  
*J. Catal.* **257** (2008) 315
17. Oxidation of 2-methyl-1-naphthol with H<sub>2</sub>O<sub>2</sub> over mesoporous Ti-MMM-2 catalyst.  
*J. Catal.* **236** (2005) 62
18. X-ray diffraction structure analysis of MCM-48 mesoporous silica.  
*J. Phys. Chem. B.* **109** (2005) 3233

The filamentous carbon material produced via decomposition of 1-iodobutane on the Ni ribbon at 600 °C



1 μm

# X-Ray Diffraction and Scattering

## X-Ray Absorption Spectroscopy: Extended X-Ray Absorption Fine Structure (EXAFS) X-Ray Absorption Near Edge Structure (XANES)

### Scientific and analytical tasks

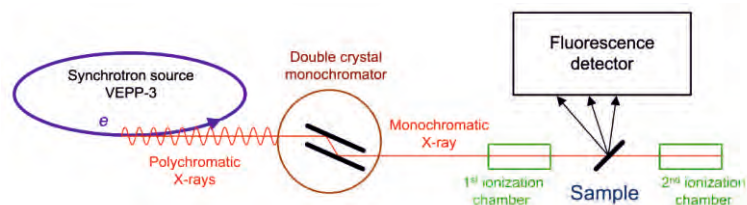
- Determination of the local geometric and electron structure of amorphous and well crystallized materials in solid or liquid state. Analysis of EXAFS spectra allows us to determine the radii of coordination spheres, coordination numbers, and Debye-Waller factors

### Equipment

EXAFS spectroscopy station consists of a monochromator based on a precision goniometer RV240-HAHLT (Newport), X-ray detectors, and an automated data acquisition system. The stations are mounted at VEPP-3 electron storage ring at Budker Institute of Nuclear Physics SB RAS

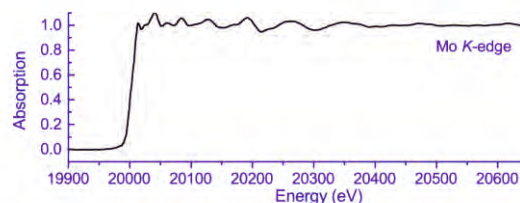
#### Station parameters:

- Energy range is 4.5 - 35 keV
- Intrinsic energy resolution ( $\Delta E/E$ ) is  $2.0 \times 10^{-4}$  for Si(111)



#### Techniques for recording spectra:

The spectra recording by total external reflection, in transmission mode and by the registration of X-ray fluorescence photons in account mode



### References

1. Support effect for nanosized Au catalysts in hydrogen production from formic acid decomposition. *Catal. Science Technol.* **6** (2016) 6853.
2. The effect of metal deposition order on the synergistic activity of Au-Cu and Au-Ce metal oxide catalysts for CO oxidation. *Applied Catalysis B* **168-169** (2014) 303.
3. Synthesis and microstructure of iridium coatings on carbon fibers. *Carbon* **56** (2013) 243.
4. Novel gold catalysts for the direct conversion of ethanol into  $C^{3+}$  hydrocarbons. *J. Catal.* **297** (2013) 296.
5. Structural changes in a nickel-copper catalyst during growth of nitrogen-containing carbon nanofibers by ethylene/ammonia decomposition. *Carbon* **48** (2010) 2792.

Platinoid gauzes containing Pt (81 wt %), Pd (15 wt %), Rh (3.5 wt %),  
and Ru (0.5 wt %) for industrial ammonia oxidation in air



500 μm

# X-Ray Diffraction and Scattering

## Small Angle X-Ray Scattering (SAXS)

### Scientific and analytical tasks

- Investigation of particle sizes, shapes, and size distributions for liquid and solid dispersed systems (supported catalysts, composite materials (including bio - and natural materials), sols, gels, crude oils, etc.)
- *In situ* study of the particle aggregation processes in liquids
- Study of ordered porous system (mesoporous oriented materials, MOF)

### Equipment

#### Diffractometer HECUS S3 Micro

- CuK $\alpha$  radiation with a point collimation
- The scattering intensity is measured in the range of the scattering vector magnitudes  $0.01 < q < 0.6 \text{ \AA}^{-1}$ . The scattering vector magnitude  $q = 4\pi \cdot \sin(\theta) / \lambda$  (where  $2\theta$  is the scattering angle, and  $\lambda = 1.541 \text{ \AA}$  is the radiation wavelength) is used as the scattering coordinate
- Possible sample heating: up to  $300 \text{ }^\circ\text{C}$
- As an additional feature a liquid masking technique can be used, which allows obtaining a scattering signal from active component in multi-component systems selectively

### References

1. Influence of a precursor solution on the characteristics of platinum on alumina catalysts. *Mendeleev Commun.* **27** (2017) 70
2. The influence of different organic solvents on the size and shape of asphaltene aggregates studied via small-angle X-ray scattering and scanning tunneling microscopy. *Adsorpt. Sci. Technol.* **34** (2016) 244
3. Study of silica templates in the rice husk and the carbon-silica nanocomposites produced from rice husk. *J. Phys. Chem. Solids* **87** (2015) 58
4. Formation of active component particles in platinum catalysts on  $\alpha$ - and  $\gamma$ -alumina. *Mendeleev Commun.* **25** (2015) 463
5. Oxidation of Ag nanoparticles in aqueous media: Effect of particle size and capping. *Appl. Surf. Sci.* **297** (2014) 75
6. Advances in SAXS for supported catalysts study. *J. Appl. Crystallogr.* **46** (2013) 752
7. Palladium-zinc catalysts on mesoporous titania prepared by colloid synthesis. I. Size control synthesis of PdZn nanoclusters by a polyol method. *J. Nanopart. Res.* **14** (2012) 1089
8. Palladium-zinc catalysts on mesoporous titania prepared by colloid synthesis. II. Synthesis and characterization of PdZn/TiO<sub>2</sub> coating on inner surface of fused silica capillary. *J. Nanopart. Res.* **14** (2012) 1088



Diffractometer HECUS S3 Micro

# Microscopy

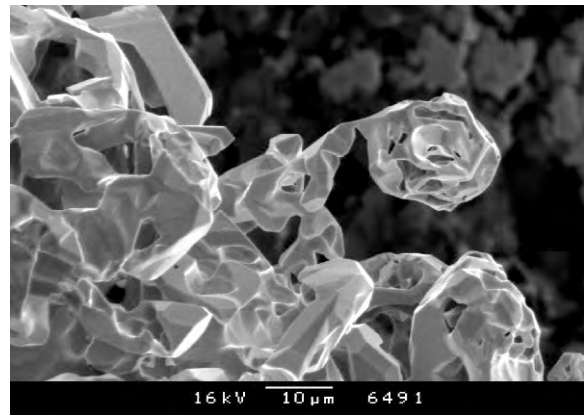
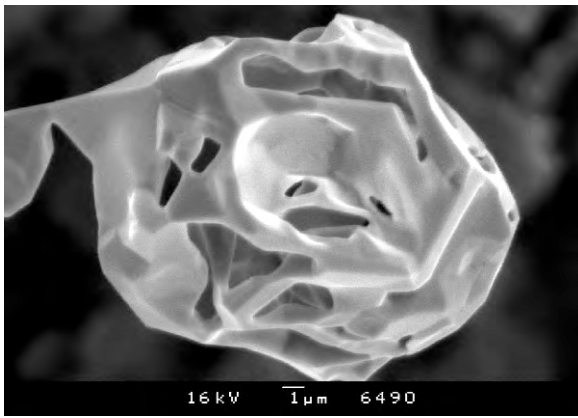
## Scanning Electron Microscopy (SEM)

### Scientific and analytical tasks

- The study of the microstructure and properties of solids, including catalyst and other functional materials using scanning electron microscopy
- The investigation of the morphology and microstructure of solid surface materials with measurement of the size of objects in the range of 50 to  $10^7$  nm in the secondary electron (SE) mode
- The study of the phase distribution on the surface and in the bulk materials, including sections (slices) of pellet catalysts in backscattering electron (BSE) mode
- The qualitative and quantitative chemical analysis using energy dispersive spectroscopy (EDS) to determine the chemical composition of the surface layers of materials with a spatial resolution of  $\leq 1$  micron. Qualitative analysis involves the identification of chemical elements from  $\text{Be}^4$  to  $\text{U}^{92}$ . Quantitative analysis allows determining the amount of chemical elements with an accuracy as high as  $\pm 1 - 2\%$  with a minimum element content of 0.1 wt.%
- Mapping of the distribution of chemical elements with analysis of phases on the surface and in the bulk materials, including sections (slices) of catalyst pellets

Scanning Electron Microscopes  
JEOL JSM-6460LV





## Equipment

### Scanning Electron Microscopes JEOL JSM-6460LV

- Resolution HV mode 3.0 nm (30 kV), 20 nm (1 kV) / LV mode 4.0 nm (30 kV)
- Magnification × 8 to × 300,000 / × 5 to × 7 available
- Preset magnifications 5 steps, user selectable
- User options Optics, Specimen stage, Image mode, LV pressure, Standard options
- Image mode Secondary electron image, Composition, Topography, Shadowed
- Accelerating voltage 0.3 kV to 30 kV
- Filament Factory pre-centered filament
- Electron gun Fully automated, manual override
- Condenser lens Zoom condenser lens
- Objective lens Super conical objective lens
- Electrical image shift ±50 μm (WD = 10 mm)
- Specimen stage Large eucentric type, X: 125 mm, Y: 100 mm, Z: 5 mm to 80 mm, Tilt: -10° to +90°, Rotation: 360°
- Specimen exchange Through the front door
- Maximum specimen 200 mm diameter × 80 mm height
- Pumping Fully automated, DP: 1. RP: 1 or 2\*
- Switching of vacuum mode Through the menu, less than 1 minute
- LV Pressure 1 to 270 Pa

## References

1. Design of functionally graded multilayer thermal barrier coatings for gas turbine application. *Surface and Coatings Technology* **295** (2016) 20
2. Structured reactors on a metal mesh catalyst for various applications. *Catalysis Today* **273** (2016) 213
3. Ceramic matrix composites prepared from CoAl powders. *Journal of Materials Science* **51** (2016) 10487
4. Effect of N and F content on structural, optical and photocatalytic methylene blue degradation properties of TiO<sub>2</sub>. *Journal of Chemical Research* **40** (2016) 729
5. Synthesis of Mg<sup>2+</sup>-, Al<sup>3+</sup>-, and Ga<sup>3+</sup>-containing layered hydroxides and supported platinum catalysts based thereon. *Kinetics and Catalysis* **57** (2016) 546
6. Phase evolution during early stages of mechanical alloying of Cu-13 wt.% Al powder mixtures in a high-energy ball mill. *Journal of Alloys and Compounds* **629** (2015) 343
7. Preparation of porous ceramometal composites through the stages of mechanical activation and hydrothermal partial oxidation of Me-Al powders. *Catalysis Today* **246** (2015) 232
8. Synthesis and physicochemical and catalytic properties of apatite-type lanthanum silicates. *Kinetics and Catalysis* **55** (2014) 361
9. Design of Al<sub>2</sub>O<sub>3</sub>/CoAlO/CoAl porous ceramometal for multiple applications as catalytic supports. *Advanced Materials Research* **702** (2013) 79
10. Catalytic combustion of brown coal particulates over ceramometal honeycomb catalyst. *Catalysis for Sustainable Energy* **1** (2013) 82
11. (CuO-CeO<sub>2</sub>)/glass cloth catalysts for selective CO oxidation in the presence of H<sub>2</sub>: The effect of the nature of the fuel component used in their surface self-propagating high-temperature synthesis on their properties. *Kinetics and Catalysis* **54** (2013) 59
12. Studies of the effect of surface modification of carbon sorbents by poly-N-vinylpyrrolidone using a complex of physicochemical and microbiological methods. *Protection of Metals and Physical Chemistry of Surfaces* **49** (2013) 430
13. Properties of porous FeAlO<sub>y</sub>/FeAl<sub>x</sub> ceramic matrix composite influenced by mechanical activation of FeAl powder. *Bulletin of Materials Science* **36** (2013) 1195
14. Relationship between composition and structure of globules in narrow fractions of ferrospheres. *Fuel* **111** (2013) 332
15. Functional nanoceramics for intermediate temperature solid oxide fuel cells and oxygen separation membranes. *Journal of the European Ceramic Society* **33** (2013) 2241
16. Formation of micro, nano and atomic-level structure of CoAlO/Co-Al cermets prepared by mechanical alloying. *Journal of Materials Science and Engineering (A & B)* **2** (2012) 121
17. Observation of room-temperature formation of carbon nanotubes as a result of the detachment of a gold nanolayer from a glass substrate. *Thin Solid Films* **520** (2012) 4174
18. Composition and properties of functional groups on surface of carbon sorbents modified by aminocaproic acid. *Protection of Metals and Physical Chemistry of Surfaces* **46** (2011) 181

The carbon material obtained by polyvinyl chloride decomposition over the bulk iron item in a closed reactor system at 600 °C



1 μm

# Microscopy

## Scanning Tunneling Microscopy (STM)

### Scientific and analytical tasks

- Visualization of the surface topography for conductive or semiconductor specimens
- Monitoring the structure alterations of model metal catalysts (catalytic corrosion, faceting, adsorbate-induced single crystal surface reconstruction, etc.)
- Detection of nanoscale topographic features (nanoparticles, pitches) at the surface of the model supports and catalysts. Evaluation of particle size distribution (optionally *in situ*)
- The studies of thermal and catalytic stability of metal nanoparticles - the active component of the supported metal catalysts

### Equipment

3 various STM machines (one - on the bench, two - UHV set-ups).

The champion is UHV 7000 VT STM (RHK, USA) - Variable Temperature (170K - 800K) UHV STM

### UHV 7000 VT STM Complete System (RHK, USA)

- Separate thermally isolated scanner and sample holder
- Scanning field of 0.5 cm<sup>2</sup>
- Max scan size - 8 × 8 × 1 mkm<sup>3</sup>. Atomic resolution at Si(7 × 7)
- Scanning Tunneling Spectroscopy measurements (recording I-V curves in predetermined positions at topographic scan)
- Exchangeable Pt-Ir cut tips (Probe exchange duration - 5+ min). Tip conditioning unit (combined radiation and e-Beam heating design)
- Three-level vibration isolation system
- e-Beam or bulb heating from the back side of the specimen. LN cooling of sample stage
- Integrated ion + sublimation pump station in STM chamber (basic pressure of 1 × 10<sup>-8</sup> Pa) Preparation and Load Lock pumping by turbomolecular pumps (residual gases pressure of 10<sup>-7</sup> Pa)
- Auxiliary equipment includes: XPS subsystem - PHOIBOS-100 MCD-5 analyzer (SPECS, Germany) and non-monochromatic AlK $\alpha$ /MgK $\alpha$  primary excitation source (up to 200 W) XR-2 (VG Scientific, UK)
- IQE 11/35 ion source for the surface cleaning by ion (Ar<sup>+</sup>, He<sup>+</sup>) etching
- e-Beam heating (up to 1000 K) and LN cooling (down to 170K) sample stages both in Analysis and Prep chambers for UHV conditions
- Irradiation (bulb) heating (up to 700 K) in the reaction mixtures at 10<sup>-3</sup> Pa (optional)

## References

1. New Pt/Alumina model catalysts for STM and *in situ* XPS studies.  
*Applied Surface Science* 401 (2017) 341
2. Using X-ray photoelectron spectroscopy to evaluate size of metal nanoparticles in the model Au/C samples.  
*The Journal of Physical Chemistry C* 120 (2016) 10419
3. XPS/STM study of model bimetallic Pd-Au/HOPG catalysts.  
*Applied Surface Science* 367 (2016) 214
4. The model thin film alumina catalyst support suitable for catalysis-oriented surface science studies.  
*Applied Surface Science* 349 (2015) 310

# Microscopy

## Transmission Electron Microscopy (TEM)

### Scientific and analytical tasks

- Investigation of a microstructure of catalysts and adsorbents using a method of transmission electron microscopy with the spatial resolution of atomic level and electron diffraction: supported metal and oxide systems, mesoporous substances, carbon nanomaterials, colloids, etc.
- Use of built-in an energy-dispersion X-ray spectrometer (with Silicon Drift Detectors for TEM) allows the element analysis of samples with localness up to 10 nanometers

### Microscope in Boreskov Institute of Catalysis

#### Equipment

#### Electron microscope JEM 2010 (JEOL Ltd., Japan)

The JEM-2010 instrument incorporates multiple additional functions such as a transmission electron microscope (TEM) image observation device and an energy dispersive X-ray spectrometer (EDS)

#### JEM 2010 Main Characteristics:

- Diffraction contrast
- High resolution image observation
- Selected area diffraction. Camera Length: 80 to 8000 mm
- EDX module, chemical analysis with locality up to 10 nm
- Accelerating voltage 200 kV
- Cathode: LaB<sub>6</sub> monocrystal
- Beam tilt:  $\pm 5^\circ$
- Minimal spot size: 1 nm
- Objective lens: Focus: 1.8 mm, Cs: 0.5 mm, Cc: 1.0 mm  
Minimal focus step: 1 nm. Type of pole piece: UD-UHR
- Stability of lens current:  $10^{-6}$
- Magnification range: 2000 to 1.5 M
- Low magnification range: 50 to 6000
- Diffraction chamber length: 80 to 1500 mm
- Point resolution: 0.194 nm
- Line resolution: 0.140 nm
- Goniometer tilt along two axes:  $\pm 15^\circ$

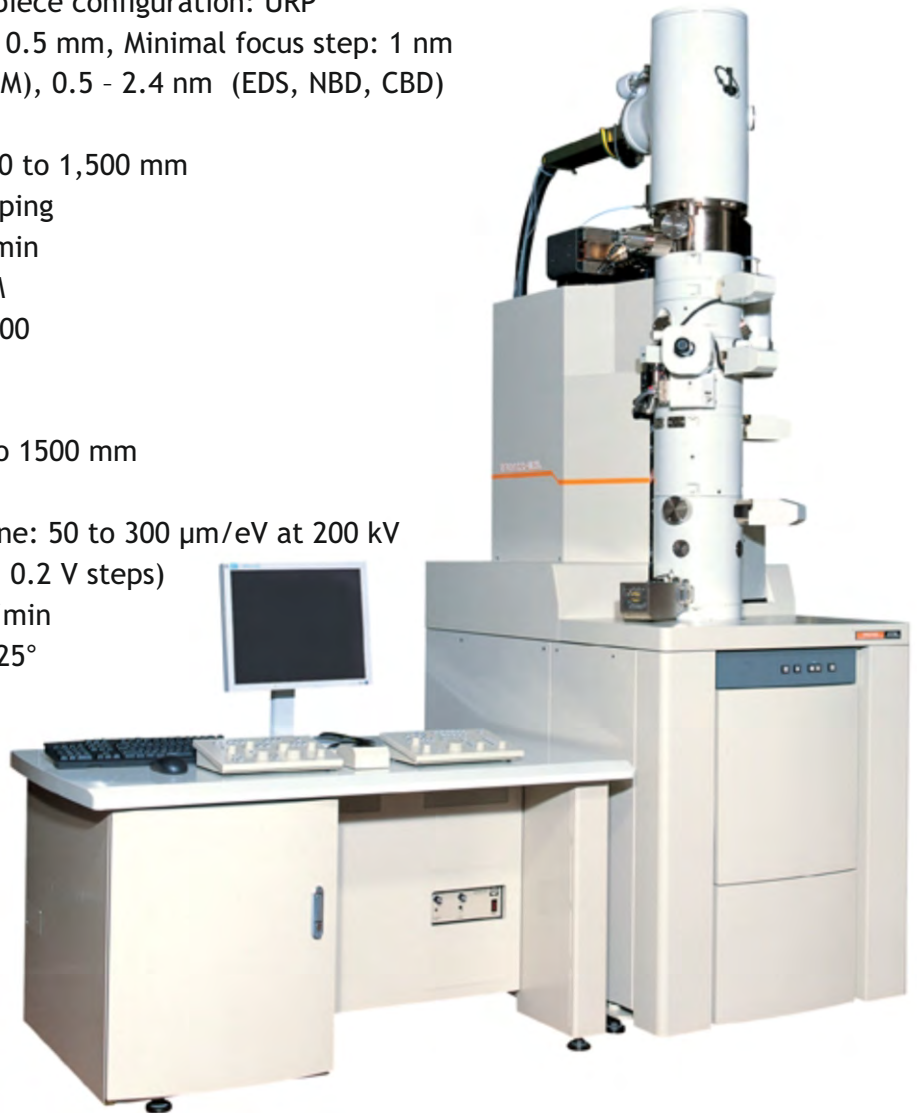


## Center of Collective Use (Novosibirsk State University)

### Field emission energy filter electron microscope JEM 2200FS with spherical aberration (Cs) corrector system (JEOL Ltd., Japan)

#### JEM-2200FS Main Characteristics:

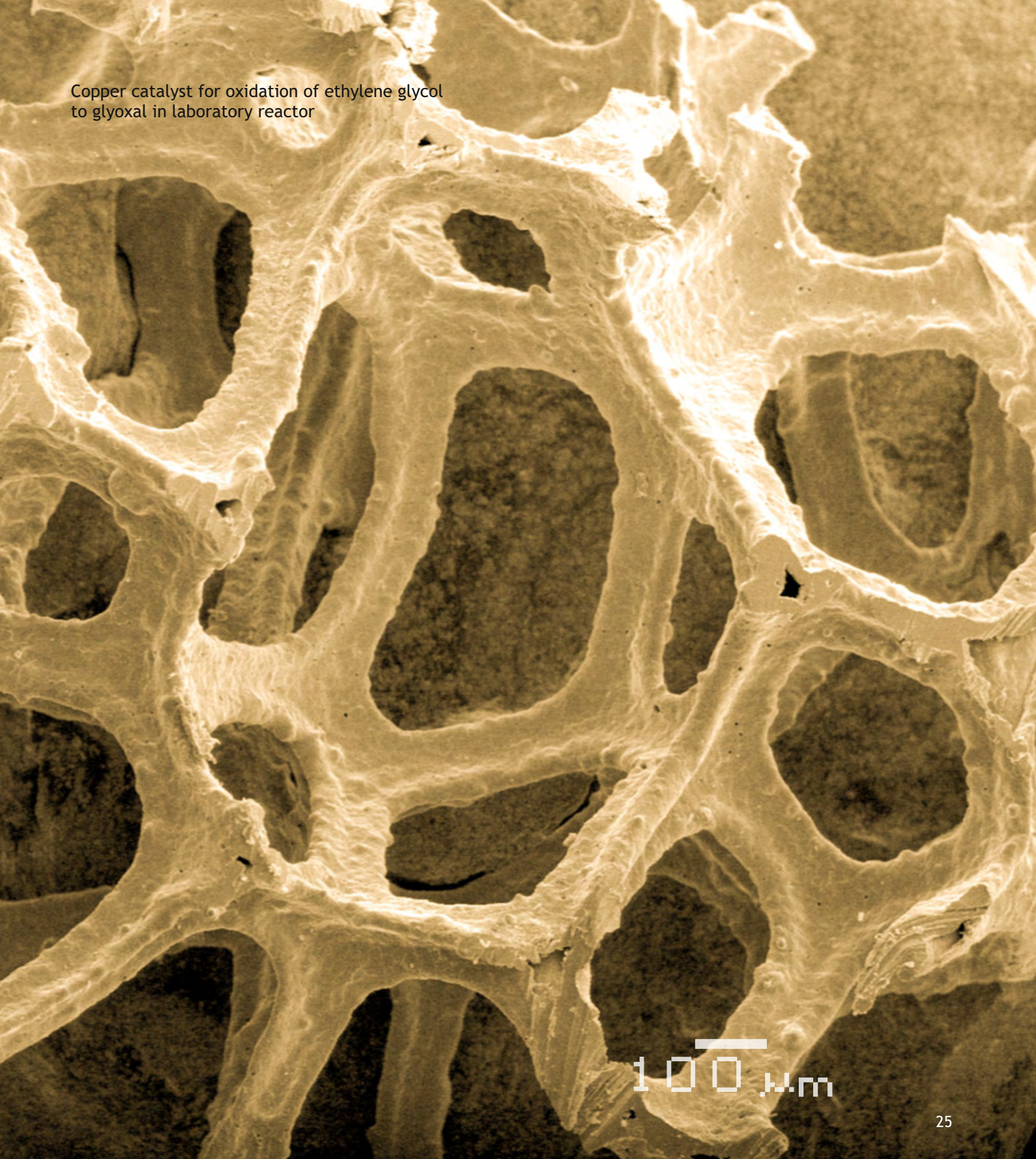
- Accelerating voltage: 200 kV
- Electron gun Schottky emitter: ZrO/W (100)
- Intensity:  $4 \times 10^8$  A/cm<sup>2</sup>/sr. or more
- Ultrahigh resolution in TEM. Pole piece configuration: URP
- Objective lens: focus 1.9 mm, Cs: 0.5 mm, Minimal focus step: 1 nm
- Spot Size (diameter): 2 - 5 nm (TEM), 0.5 - 2.4 nm (EDS, NBD, CBD)
- STEM mode. Detectors: HAADF, BF
- SA diffraction, Camera Length: 150 to 1,500 mm
- EDS: JED-2300T, from B to U, mapping
- Stability of lens current:  $1 \times 10^{-6}$ /min
- Magnification range: 2000 to 1.5 M
- Low magnification range: 50 to 1500
- Point resolution: 0.19 nm
- Line resolution: 0.1 nm
- Diffraction chamber length: 150 to 1500 mm
- EELS energy resolution: 0.8 eV
- EELS dispersion on final image plane: 50 to 300  $\mu\text{m}/\text{eV}$  at 200 kV
- Energy shift 3,000 V, maximum (in 0.2 V steps)
- Stability of filter current:  $1 \times 10^{-6}$ /min
- Goniometer tilt along two axes:  $\pm 25^\circ$



## References

1. The effect of oxidative and reductive treatments of titania-supported metal catalysts on the pairwise hydrogen addition to unsaturated hydrocarbons.  
*Catal. Today* **283** (2017) 82
2. Coherent 3D nanostructure of  $\gamma$ - $\text{Al}_2\text{O}_3$ : Simulation of whole X-ray powder diffraction pattern.  
*J. Solid State Chem.* **246** (2017) 284
3. Study of catalyst deactivation in liquid-phase hydrogenation of 3-nitrostyrene over Au/ $\text{Al}_2\text{O}_3$  catalyst in flow reactor.  
*Catal. Letters* (2017) DOI: 10.1007/s10562-016-1959-3
4. N-Lauroylsarcosine capped silver nanoparticle based inks for flexible electronics.  
*J. Mater. Sci. - Mater. Electron.* **28** (2017) 2029
5. Influence of boron addition to alumina support by kneading on morphology and activity of HDS catalysts.  
*Appl. Catal., B* **199** (2016) 23
6. Microstructural changes in  $\text{La}_{1-x}\text{Ca}_x\text{CoO}_{3-\delta}$  solid solutions under the influence of catalytic reaction of methane combustion.  
*Top. Catal.* **59** (2016) 1354
7. Synthesis of  $\text{Pt}/\text{Zn}(\text{OH})_2/\text{Cd}_{0.3}\text{Zn}_{0.7}\text{S}$  for the photocatalytic hydrogen evolution from aqueous solutions of organic and inorganic electron donors under visible light.  
*Top. Catal.* **59** (2016) 1297
8. Catalysts based on amorphous aluminosilicates for selective hydrotreating of FCC gasoline to produce Euro-5 gasoline with minimum octane number loss.  
*Catal. Today* **271** (2016) 4
9. CoNiMo/ $\text{Al}_2\text{O}_3$  catalysts for deep hydrotreatment of vacuum gasoil.  
*Catal. Today* **271** (2016) 56
10. Silver sulfide nanoparticles with a carbon-containing shell.  
*Inorg. Mater.* **52** (2016) 441
11. Novel photocatalysts  $\text{Pt}/\text{Cd}_{1-x}\text{Zn}_x\text{S}/\text{ZnO}/\text{Zn}(\text{OH})_2$ : Activation during hydrogen evolution from aqueous solutions of ethanol under visible light.  
*Appl. Catal., B* **183** (2016) 197
12. Structure and morphology evolution of silica-modified pseudoboehmite aerogels during heat treatment.  
*J. Solid State Chem.* **233** (2016) 294
13. Nanocrystalline ordered vanadium carbide: Superlattice and nanostructure.  
*Superlattices Microstruct.* **90** (2016) 148
14. Study on thermal decomposition of double complex salt  $[\text{Pd}(\text{NH}_3)_4][\text{PtCl}_6]$ .  
*J. Therm. Anal. Calorim.* **123** (2016) 1183
15. Low- and high-temperature oxidation of  $\text{Mn}_{1.5}\text{Al}_{1.5}\text{O}_4$  in relation to decomposition mechanism and microstructure.  
*Cryst. Eng. Comm.* **18** (2016) 3411
16. Electrostatic origin of stabilization in  $\text{MoS}_2$ -organic nanocrystals.  
*J. Phys. Chem. Letters* **7** (2016) 516
17. Electrocatalysis of the hydrogen oxidation reaction on carbon-supported bimetallic NiCu particles prepared by an improved wet chemical synthesis.  
*J. Electroanal. Chem.* **783** (2016) 146
18. The effect of support pretreatment on activity of Ag/ $\text{SiO}_2$  catalysts in low-temperature CO oxidation.  
*Catal. Today* **278** (2016) 150
19. Ethanol dehydrogenation over Ag- $\text{CeO}_2$ / $\text{SiO}_2$  catalyst: Role of Ag- $\text{CeO}_2$  interface.  
*Appl. Catal., A* **528** (2016) 161
20. Modifying magnetic properties and dispersity of few-layer  $\text{MoS}_2$  particles by 3d metal carboxylate complexes.  
*Mater. Chem. Phys.* **183** (2016) 457
21. XPS study of nanostructured rhodium oxide film comprising  $\text{Rh}^{+}$  species.  
*J. Phys. Chem. C* **120** (2016) 19142
22. Bone-like hydroxyapatite formation in human blood.  
*Int. J. Environ. Sci. Education* **11** (2016) 3971
23. Zinc influence on the formation and properties of Pt/Mg(Zn)AlO<sub>x</sub> catalysts synthesized from layered hydroxides.  
*J. Catal.* **41** (2016) 13
24. Facile synthesis of gold nanoparticles in aqueous acrylamide solution.  
*Rus. J. Inorganic Chem.* **61** (2016) 535
25. Versatile PdTe/C catalyst for liquid-phase oxidations of 1,3-butadiene.  
*Appl. Catal., A* **513** (2016) 30
26. Identification of  $\epsilon$ - $\text{Fe}_2\text{O}_3$  nano-phase in borate glasses doped with Fe and Gd.  
*J. Magn. Magn. Mater.* **401** (2016) 880
27. Pd/C catalysts based on synthetic carbons with bi- and tri-modal pore-size distribution: Applications in flow chemistry.  
*Catal. Sci. Technol.* **6** (2016) 2387
28. Modern electron microscopy in the study of chemical systems at the boundary of organic synthesis and catalysis.  
*Russ. Chem. Rev.* **85** (2016) 11, 1198-1214 DOI: <https://doi.org/10.1070/RCR4681>

Copper catalyst for oxidation of ethylene glycol  
to glyoxal in laboratory reactor



100  $\mu\text{m}$

# Surface Science

## X-Ray Photoelectron Spectroscopy (XPS)

## Electron Spectroscopy for Chemical Analysis (ESCA)

### Scientific and analytical tasks

- Elemental analysis (except for H) of both the surface composition of solids and adsorbed layers (at bulk specimens). Investigation of chemical states of the detected elements as well as *in situ* monitoring of its alterations. Depth profiling measurements - either during ion etching (destructive) or by application of the alternative X-ray excitation and Angle Resolved XPS (non-destructive)
- The studies (including *in situ*) of the active sites composition and chemical states of the model bulk (single crystals and foils) and supported metal and metal-oxide catalysts for total or partial hydrocarbon and CO oxidation, DeNO<sub>x</sub>, etc. to achieve the solution of the following scientific tasks:
  - exploration on the effects of catalyst elemental composition, structure and reaction conditions on the rate of catalytic reactions
  - understanding of the catalyst active sites nature, surface states and other peculiarities of the detailed mechanism of catalytic reactions
  - the studies of thermal and catalytic stability of metal nanoparticles - the active component of the supported metal catalysts
  - development of synthesis and activation protocols to prepare the improved supported metal catalysts
- Chemical analysis of the multi-phase composites utilized in semiconductors, fuel cells, etc.
- Evaluation of chemical composition and amounts of biologically important species (proteins, polysaccharides, etc.) anchored at the surface of biodegradable substrates

### Equipment

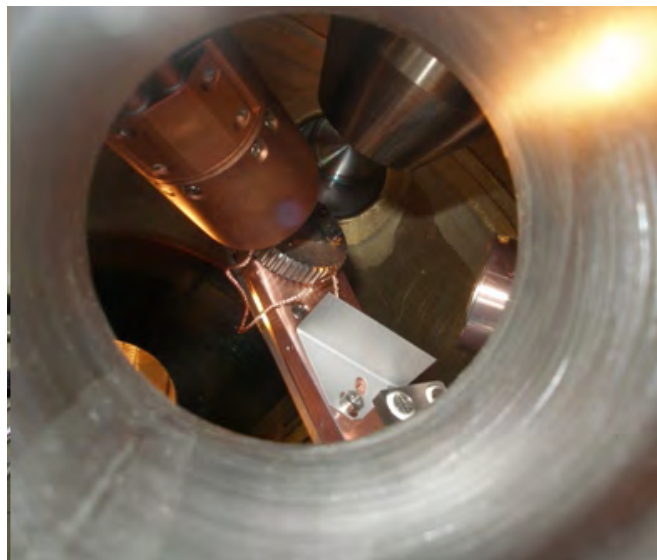
6 various experimental machines equipped with XPS.

The flagship is PHOIBOS-150 MCD-9 spectrometer (SPECS, Germany)

#### PHOIBOS-150 MCD-9 electron spectrometer (SPECS, Germany)

- 9 channeltrons detector (up to  $3 \times 10^6$  cps)
- Monochromatic AlK $\alpha$ /AgL $\alpha$  and non-monochromatic AlK $\alpha$ /MgK $\alpha$  primary excitation sources (up to 400 W). Flood Gun FG 15/40
- Turbomolecular pumping 4 chambers set up (residual gases pressure of  $10^{-7} \div 10^{-8}$  Pa)
- IQE 11/35 ion source for the surface cleaning by ion (Ar<sup>+</sup>, He<sup>+</sup>) etching
- e-Beam heating (up to 1000 K) and LN cooling (down to 170 K) sample stages both in Analysis and Prep chambers for UHV conditions

- Irradiation (bulb) heating (up to 700K) in the reaction mixtures at  $10^{-3}$  Pa (optionally)
- Omicron EFM-3 evaporator for thermal vacuum deposition of metal particles / layers (optionally)
- High Pressure cell for the sample treatments (up to 700 K at 3 bar)
- He / ultra pure nitrogen filled Glove Box sample loading system (optionally)



## References

1. Human serum albumin in electrospun PCL fibers: Structure, release, and exposure on fiber surface. *Polymers for Advanced Technologies* (2016) DOI: 10.1002/pat.3984
2. Zinc influence on the formation and properties of Pt/Mg(Zn)AlO<sub>x</sub> catalysts synthesized from layered hydroxides. *J. Catal.* **341** (2016) 13
3. Ferromagnetic HfO<sub>2</sub>/Si/GaAs interface for spin-polarimetry applications. *Appl. Phys. Lett.* **107** (2015) 123506-1
4. Effect of the nature of carbon support on the formation of active sites in Pd/C and Ru/C catalysts for hydrogenation of furfural. *Catal. Today.* **249** (2015) 145
5. Effect of calcination temperature on the properties of Pt/SAPO-31 catalyst in one-stage transformation of sunflower oil to green diesel. *Appl. Catal. A: General* **505** (2015) 524
6. Interaction of SO<sub>2</sub> with Pt model supported catalysts studied by XPS. *J. Phys. Chem. C.* **118** (2014) 22120
7. Ni-based sol-gel catalysts as promising systems for crude bio-oil upgrading: Guaiacol hydrodeoxygenation study. *Appl. Catal., B: Environmental* **113** (2012) 296
8. Optimization of Ni<sup>2+</sup>/Ni<sup>3+</sup> ratio in layered Li(Ni, Mn, Co)O<sub>2</sub> cathodes for better electrochemistry. *J. Power Sources* **174** (2007) 965
9. Synthesis and structural characterization of Se-modified carbon-supported Ru nanoparticles for the oxygen reduction reaction. *J. Phys. Chem. B.* **110** (2006) 6881
10. Interaction of Al<sub>2</sub>O<sub>3</sub> and CeO<sub>2</sub> surfaces with SO<sub>2</sub> and SO<sub>2</sub>+O<sub>2</sub> studied by X-ray photoelectron spectroscopy. *J. Phys. Chem. B.* **109** (2005)

# Surface Science

## High Pressure X-Ray Photoelectron Spectroscopy (HP XPS)

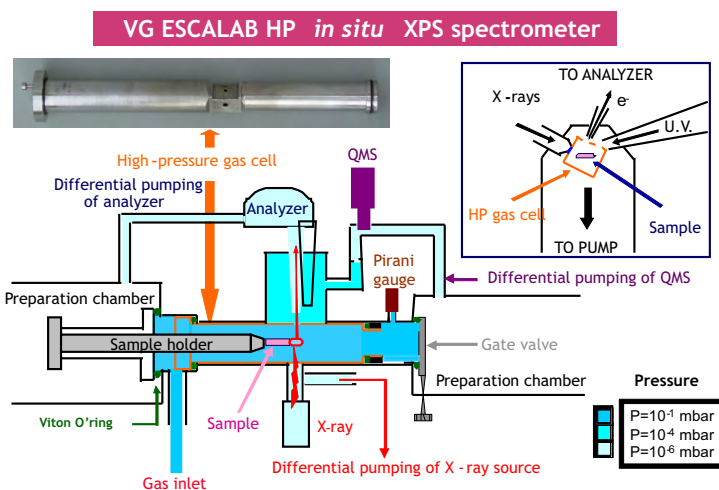
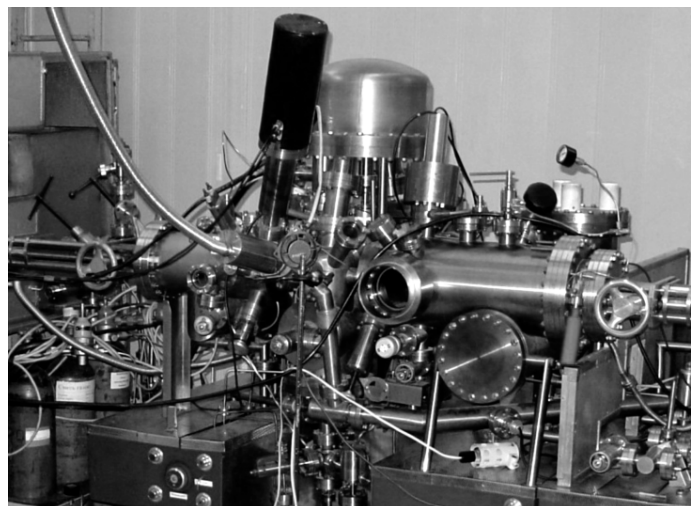
### Scientific and analytical tasks

- Elemental analysis (except for H) of both the surface composition of solids and adsorbed layers (at bulk specimens). Investigation of chemical states of the detected elements as well as *in situ* monitoring of their alterations at elevated (up to 20 Pa) reaction mixture pressure over the specimen
- The studies (including *in situ*) of the active sites composition and chemical states of the model bulk (single crystals and foils) and supported metal and metal-oxide catalysts for total or partial hydrocarbon and CO oxidation, DeNO<sub>x</sub>, etc. to achieve the solution of the following scientific tasks:
  - exploration on the effects of catalyst elemental composition, structure and reaction conditions on the rate of catalytic reactions
  - understanding of the nature of the catalyst active sites, surface states and other peculiarities of the detailed mechanism of catalytic reactions
  - the studies of thermal and catalytic stability of nanoparticles of the active component of the supported metal catalysts
  - development of synthesis and activation protocols to prepare the improved supported metal catalysts

### Equipment

#### VG ESCALAB High Pressure electron spectrometer (VG Scientific, UK)

- Differentially pumped hemispherical electron analyzer (up to  $3 \times 10^5$  cps)
- Non-monochromatic AlK $\alpha$ /MgK $\alpha$  primary excitation source XR-3 (up to 300 W) with by-pass pumping line
- Diffusion oil pumps with LN traps in each of 4 chambers (residual gases pressure of  $10^{-7} \div 3 \times 10^{-8}$  Pa)
- Resistive heating of the specimen spot-welded to sample holder (up to 1300 K in UHV). Modified resistive heating set up for sample treatment in reaction mixtures (up to 900 K at 20 Pa)
- Detachable high pressure cell (volume < 0.5 L) acting as continuous flow reactor (optionally)
- 3 flow-mass controllers (10 mL/min) and Baratron pressure meter to produce stable feed reaction mixture
- Quadrupole mass-spectrometer (200 m.e.) Pfeiffer Prisma within by-pass pumping line for the analysis reaction cell gas phase during temperature-programmed reaction experiments. Alternatively, in UHV conditions thermodesorption spectroscopy measurements could be performed (at specimen heating rates up to 20 K/s)
- Omicron EFM-3 evaporator for thermal vacuum deposition of metal particles / layers (optionally)
- AG-3 ion source for the surface cleaning by ion (Ar<sup>+</sup>, He<sup>+</sup>) sputtering



## References

1. Perovskite-like catalysts LaBO<sub>3</sub> (B = Cu, Fe, Mn, Co, Ni) for wet peroxide oxidation of phenol.  
*Appl. Catal. B: Environmental* **180** (2016) 86
2. CoNiMo/Al<sub>2</sub>O<sub>3</sub> catalysts for deep hydrotreatment of vacuum gasoil.  
*Catal. Today* **271** (2016) 56
3. Evolution of self-sustained kinetic oscillations in the catalytic oxidation of propane over a nickel foil.  
*J. Catal.* **334** (2016) 23
4. The “direct” synthesis of trialkoxysilanes: New data for understanding the processes of the copper-containing active sites formation during the activation of the initial silicon based contact mass.  
*J. Catal.* **338** (2016) 143
5. Influence of boron addition to alumina support by kneading on morphology and activity of HDS catalysts.  
*Appl. Catal. B: Environmental* **199** (2016) 23
6. Controlled synthesis of PVP-based carbon-supported Ru nanoparticles: Synthesis approaches, characterization, capping agent removal and catalytic behavior.  
*Catal. Science Technol.* **6** (2016) 8490
7. Parahydrogen-induced polarization (PHIP) in heterogeneous hydrogenations over bulk metals and metal oxides.  
*Chem. Commun.* **50** (2014) 875
8. Evaluation of the mechanism of heterogeneous hydrogenation of alpha, beta-unsaturated carbonyl compounds via pairwise hydrogen addition.  
*ACS Catal.* **4** (2014) 2022
9. Growth of nitrogen-doped carbon nanotubes and fibers over a gold-on-alumina catalyst.  
*Carbon* **50** (2012) 1186
10. Gold nanoparticles supported on magnesium oxide as catalysts for the aerobic oxidation of alcohols under alkali free conditions.  
*J. Catal.* **292** (2012) 148
11. The silver-oxygen system in catalysis: New insights by near ambient pressure X-ray photoelectron spectroscopy.  
*Phys. Chem. Chem. Phys.* **14** (2012) 4554
12. Metal-support interactions in Pt/Al<sub>2</sub>O<sub>3</sub> and Pd/Al<sub>2</sub>O<sub>3</sub> catalysts for CO oxidation.  
*Appl. Catal., B* **97** (2010)
13. Platinum nanoparticles on Al<sub>2</sub>O<sub>3</sub>: Correlation between the particle size and activity in total methane oxidation.  
*J. Catal.* **268** (2009) 60
14. Structure and electrical conductivity of nitrogen-doped carbon nanofibers.  
*Carbon* **47** (2009) 1922
15. Nanodispersed Au/Al<sub>2</sub>O<sub>3</sub> catalysts for low-temperature CO oxidation: Results of research activity at the Boreskov Institute of Catalysis.  
*Catal. Today* **144** (2008) 292

# Surface Science

## Polarization Modulation InfraRed Reflection Absorption Spectroscopy (PM IRRAS)

### Scientific and analytical tasks

- **Operando** study of the mechanisms of heterogeneous catalytic reaction over single-crystal model catalysts by IR spectroscopy and mass spectrometry in a wide pressure range from UHV to 1 bar; to identify surface intermediates and products in the gas phase
- **In situ** study of adsorption of simple molecules on single-crystal model catalysts in a wide temperature range between 80 and 1000 K in vacuum or at ambient pressure
- **In situ** preparation and characterization of thin films or nanoparticles on the surface of single-crystal model catalysts
- Investigation of surface composition of bimetallic systems using X-ray photoelectron spectroscopy and FTIR analysis of adsorbed probe molecules

### Equipment

#### FT-IR Spectrometer VERTEX 80v (Bruker, Germany)

- Spectral range 850 - 8000  $\text{cm}^{-1}$  (liquid  $\text{N}_2$  cooled MCT detector)
- Standard spectral resolution better than 0.2  $\text{cm}^{-1}$
- Nominal modulation frequency of the IR beam polarization 42 kHz
- Pressure range in catalytic cell equipped by  $\text{BaF}_2$  windows during **operando** study between  $10^{-7}$  mbar and 1 bar. The cell is equipped with a gas inlet system ( $\text{CO}$ ,  $\text{O}_2$ , Ar,  $\text{H}_2\text{O}$ , and ethanol)

#### X-ray photoelectron spectrometer based on a PHOIBOS 150 hemispherical analyzer with a MCD-9 multichannel detector (SPECS Surface Nano Analysis, Germany)

- Non-monochromatic Mg K $\alpha$  (1256.6 eV) and Al K $\alpha$  (1486.6 eV) X-ray sources
- Sample temperature in the range between 80 and 1200 K
- Background pressure better than  $10^{-9}$  mbar

#### E-Beam Evaporator EBE-1 (SPECS Surface Nano Analysis, Germany) for deposition of films with different chemical composition or metal nanoparticles

### References

1. CO adsorption on reconstructed Ir(100) surfaces from UHV to mbar pressure: A LEED, TPD, and PM-IRAS study. *J. Phys. Chem. C* **120** (2016) 10838



# Magnetic Resonance

## Nuclear Magnetic Resonance (NMR) Spectroscopy

### Scientific and analytical tasks

#### *Homogeneous catalysis:*

- The multinuclear NMR spectroscopic study of the structure and reactivity of transition metal complexes - the active species of homogeneous catalytic oxidation and polymerization
- Analysis of complex mixtures of the products of catalytic transformations by means of  $^1\text{H}$  and  $^{13}\text{C}$  NMR spectroscopy. The control of the process of organic and organometallic synthesis of the catalysts. Analysis of the structure of copolymers of ethylene and propylene with  $\alpha$ -olefins

#### *Heterogeneous catalysis:*

- Study of the structure of the active surface sites of solid catalysts (bulk and supported) by modern multinuclear SSNMR spectroscopy (MAS with rotation frequencies up to 70 kHz, SATRAS, MQMAS, MASSA, TRAPDOR, HETCOR, CPMAS)
- NMR-crystallography approach merging state-of-the-art multinuclear SSNMR spectroscopy with state-of-the-art DFT computations (GIPAW)
- NMR of alloys (up to 650 °C)
- Internal field  $^{59}\text{Co}$  NMR
- $^{129}\text{Xe}$  NMR of adsorbed xenon

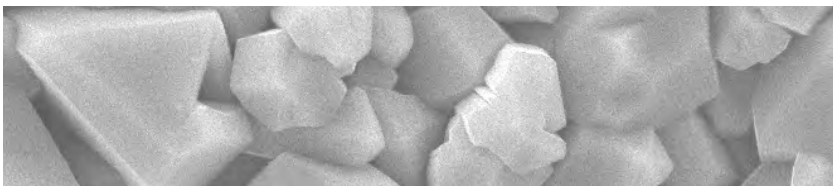
### Equipment

#### **Bruker AVANCE-400 (magnetic field 9.4 T) NMR spectrometers for liquid-state and solid-state spectroscopy with a representative set of probe heads for any applications**

- high-resolution probeheads for liquids for the whole range of frequencies; BRUKER BBO W1 5 mm and BBO W1 10 mm
- broadband high-power probeheads for the whole range of frequencies and temperatures from +300 to -150 °C; C BRUKER HP WB 73 A/BB SOL10 HT
- multinuclear X/ $^1\text{H}$  dual-channel probe heads for cross-polarization/magic angle spinning (CP/MAS) experiments BRUKER:
  - HP WB 73B MAS 7Bl CP WVT: rotation frequency up to 7 kHz
  - HP WB 73B(A) MAS 4Bl CP WVT: rotation frequency up to 15 kHz

## Additional features

- Home-built high-temperature (up to 600 °C) probe heads for studies of molten state
- High-speed MAS probes BRUKER WB CP
- HP WB 73 MAS 2.5Bl CP DVT: rotation frequency up to 35 kHz
- HP WB 73 MAS 1.3Bl CP DVT: rotation frequency up to 70 kHz
- Solid-state NMR technique for quadrupolar nuclei with a half-integral spin
- SATRAS - Satellite TRANSition Spectroscopy
- MQMAS - Multiple-Quantum MAS NMR
- MASSA - Magic Angle Spinning and Static Spectra Analysis

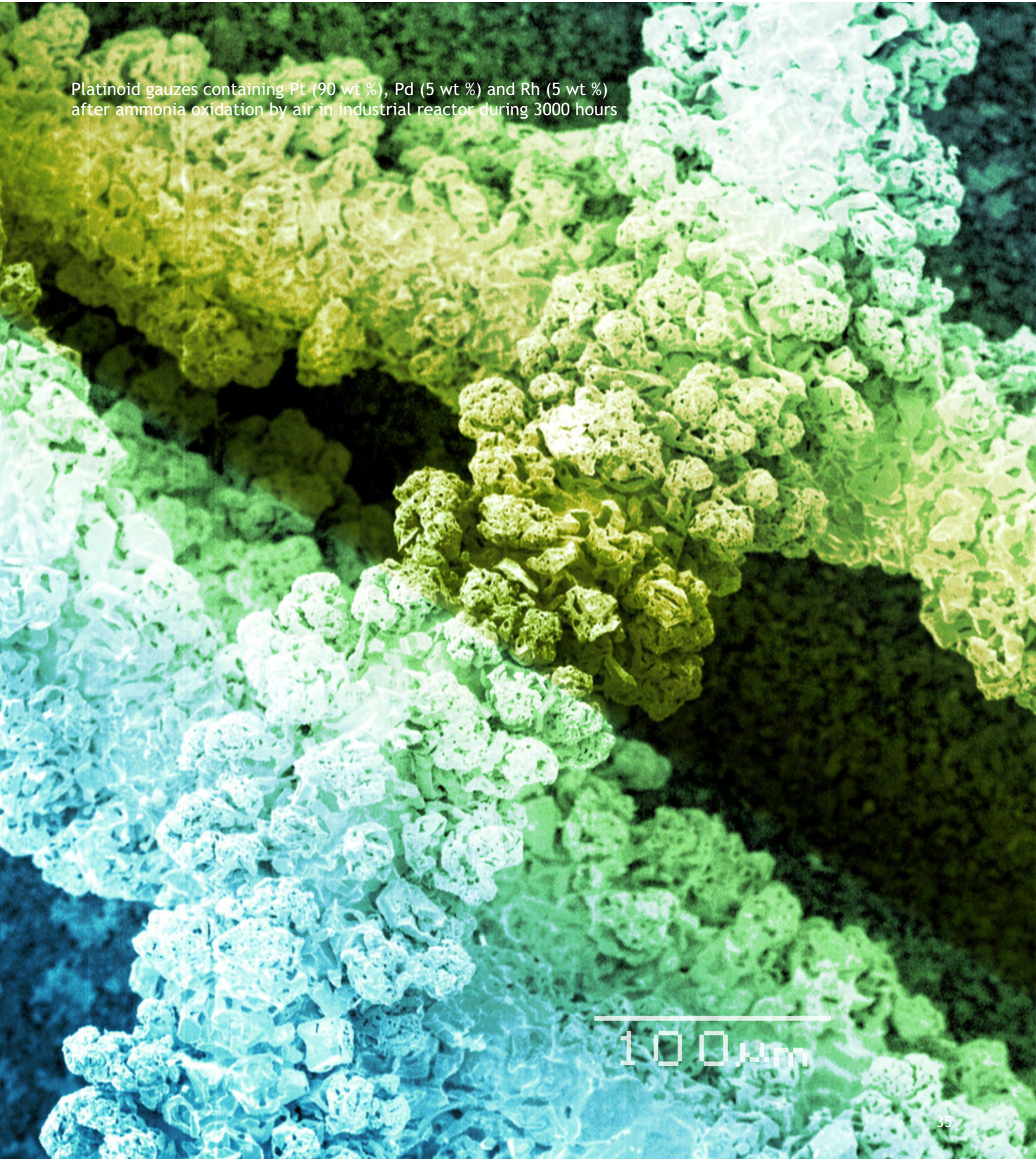


## References

1. Applications of EPR and NMR spectroscopy in homogeneous catalysis. Boca Raton, Florida: CRC Press, 2017, 222 pages. ISBN 9781498742634
2. Magnetic and dielectric properties of carbon nanotubes with embedded cobalt nanoparticles. *Carbon* 114 (2017) 39
3. Surface hydroxyl OH defects of  $\eta$ -Al<sub>2</sub>O<sub>3</sub> and  $\chi$ -Al<sub>2</sub>O<sub>3</sub> by solid state NMR, XRD, and DFT calculations. *Int. J. Res. Phys. Chem. Chem. Phys.* 231(4) (2017) 809
4. Enantioselective epoxidations of olefins with various oxidants on bioinspired Mn complexes: Evidence for different mechanisms and chiral additive amplification. *ACS Catal.* 6 (2016) 979
5. Dramatic effect of carboxylic acid on the electronic structure of the active species in Fe(PDP)-catalyzed asymmetric epoxidation. *ACS Catal.* 6 (2016) 5399
6. Modern ssNMR for heterogeneous catalysis. *Catal. Today* (2016) DOI 10.1016/j.cattod.2016.11.005
7. Random distribution of EFG parameters in <sup>27</sup>Al MAS NMR spectra of AlO<sub>x</sub>/SiO<sub>2</sub> catalysts and related systems. *Appl. Magn. Reson.* 47 (2016) 1193
8. Mechanism of selective C-H hydroxylation mediated by manganese aminopyridine enzyme models. *ACS Catal.* 5 (2015) 39

9. Effect of impregnation on the structure of niobium oxide/alumina catalysts studied by multinuclear solid-state NMR, FTIR, and quantum chemical calculations.  
*J. Phys. Chem. C* **119** (2015) 10400
10. Thermal stability and hcp-fcc allotropic transformation in supported Co metal catalysts probed near *operando* by ferromagnetic NMR.  
*Phys. Chem. Chem. Phys.* **17** (2015) 14598
11. Isoinversion behavior in the enantioselective oxidations of pyridylmethylthio benzimidazoles to chiral proton pump inhibitors on titanium salen complexes.  
*ACS Catal.* **5** (2015) 4673
12. EPR spectroscopic detection of the elusive Fe(V)=O intermediates in selective catalytic oxofunctionalizations of hydrocarbons mediated by biomimetic ferric complexes.  
*ACS Catal.* **5** (2015) 2702
13. A new insight into cobalt metal powder internal field  $^{59}\text{Co}$  NMR spectra.  
*Appl Magn Reson.* **45**(10) (2014) 1009
14. Active sites and mechanisms of bioinspired oxidation with  $\text{H}_2\text{O}_2$ , catalyzed by non-heme Fe and related Mn complexes.  
*Coord. Chem. Rev.* **276** (2014) 73
15. Highly enantioselective bioinspired epoxidation of electron-deficient olefins with  $\text{H}_2\text{O}_2$  on aminopyridine Mn catalysts.  
*ACS Catal.* **4** (2014) 1599
16.  $^1\text{H}$  and  $^2\text{H}$  NMR spectroscopic characterization of heterobinuclear ion pairs formed upon the activation of bis(imino)pyridine vanadium(III) precatalysts with  $\text{AlMe}_3/[\text{Ph}_3\text{C}]^+[\text{B}(\text{C}_6\text{F}_5)_4]^-$  and MAO.  
*Organometallics* **33** (2014) 2583
17. Formation of cationic intermediates upon the activation of bis(imino)pyridine nickel catalysts.  
*Organometallics* **32** (2013) 2187
18. Theoretical and experimental insights into applicability of solid-state  $^{93}\text{Nb}$  NMR in catalysis.  
*PCCP* **15**(14) (2013) 5115
19. Formation of trivalent zirconocene complexes from ansa-zirconocene-based olefin-polymerization precatalysts: An EPR- and NMR-spectroscopic study.  
*J. Am. Chem. Soc.* **135** (2013) 10710
20. Chemo- and stereoselective C-H oxidations and epoxidations/cis-dihydroxylations with  $\text{H}_2\text{O}_2$ , catalyzed by non-heme iron and manganese complexes.  
*Coord. Chem. Rev.* **256** (2012) 1418
21. Asymmetric epoxidations with  $\text{H}_2\text{O}_2$  on Fe and Mn aminopyridine catalysts: Probing the nature of active species by combined electron paramagnetic resonance and enantioselectivity study.  
*ACS Catal.* **2** (2012) 1196
22. Iron-catalyzed enantioselective epoxidations with various oxidants: Evidence for different active species and epoxidation mechanisms.  
*ACS Catal.* *accepted*. DOI: 10.1021/acscatal.6b02851 <http://pubs.acs.org/doi/abs/10.1021/acscatal.6b02851>
23. Highly efficient, regioselective, and stereospecific oxidation of aliphatic C-H groups with  $\text{H}_2\text{O}_2$ , catalyzed by aminopyridine manganese complexes.  
*Org. Lett.* **14** (2012) 4310
24. Frontiers of mechanistic studies of coordination polymerization and oligomerization of alpha-olefins.  
*Coord. Chem. Rev.* **256** (2012) 2994
25. The origin of living polymerization with an o-fluorinated catalyst: NMR spectroscopic characterization of chain-carrying species.  
*Chem. Eur. J.* **18** (2012) 848
26. Solid-State NMR of Oxide-Based Materials.  
*Modern Magnetic Resonance, 2nd edition, p.1-40. Springer International Publishing Switzerland 2016, G.A. Webb (ed.)*
27. Quadrupolar metal NMR of oxide materials including catalysts, chapter 27 in NMR of quadrupolar nuclei in solid materials.  
*John Wiley & Sons, Inc.*, 2012. T.27. P.467-494. ISBN 978-0-470-97398-1
28. Quadrupolar metal NMR of oxide materials including catalysts, encyclopedia of magnetic resonance.  
*John Wiley & Sons, Ltd.*, 2011. P. 1
29. Practical aspects of  $^{51}\text{V}$  and  $^{93}\text{Nb}$  solid-state NMR spectroscopy and applications to oxide materials.  
*Prog. Nucl. Magn. Reson. Spectrosc.* **53** (2008) 128

Platinoid gauzes containing Pt (90 wt %), Pd (5 wt %) and Rh (5 wt %) after ammonia oxidation by air in industrial reactor during 3000 hours



100 μm

# Magnetic Resonance

## *In Situ* Magic Angle Spinning Nuclear Magnetic Resonance (MAS NMR) Spectroscopy

### Scientific and analytical tasks

- Characterization of solids (qualitative and quantitative analysis, chemical environment of a given atomic nucleus on the basis of characteristic chemical shifts in the NMR spectrum)
- *In situ* investigation of chemical reactions under continuous flow and static conditions, identification of the nature and structure for intermediates and products during chemical transformation of the adsorbed substances, kinetic measurements, monitoring of the selective isotope labels ( $^{13}\text{C}$ ,  $^2\text{H}$ ,  $^{15}\text{N}$ ) redistribution in molecules, determination of the mechanisms of chemical reactions
- Study of the molecular dynamics by modeling of  $^2\text{H}$  NMR spectra and temperature dependence of the relaxation times  $T_1$ ,  $T_2$  (peculiarities of molecular mobility in solids or adsorbed molecules)

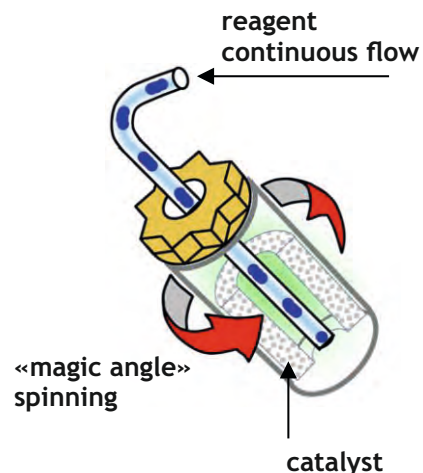
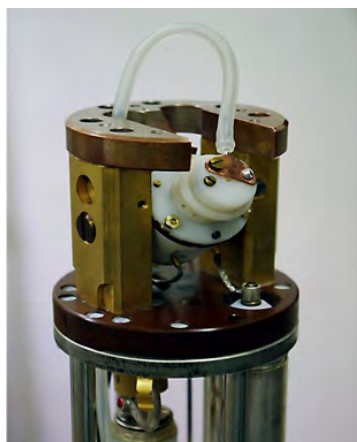
### Equipment

#### NMR spectrometer Bruker Avance-400

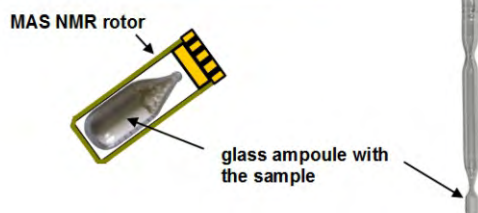
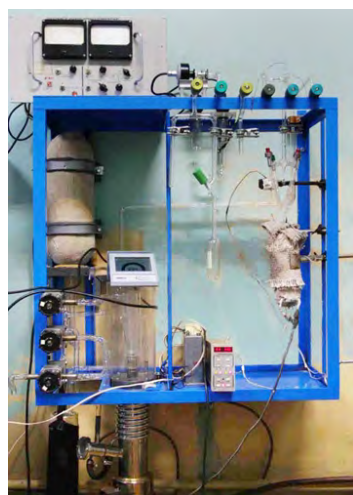
- Ultrashield cryomagnet 9.4 T
- Fourier-NMR spectrometer
- Two RF channels (nuclei X,  $^1\text{H}$ ) with high-power (1 kW) amplifiers
- Broad-band NMR probes with X-channel frequencies spanned from  $^{105}\text{Pd}$  (18.3 MHz) to  $^{31}\text{P}$  (161.9 MHz)
- Pneumatic MAS unit for registering NMR spectra with rotation under magic angle, MAS NMR probes with rotor's diameter 7, 4, 2.5, 1.3 mm (max speed of rotation 7, 18, 35, 67 kHz, correspondingly)
- Temperature unit BVT 3000, temperature range from  $-140\text{ }^\circ\text{C}$  to  $+300\text{ }^\circ\text{C}$ , precision of temperature adjustment  $0.1\text{ }^\circ\text{C}$
- Sample preparation system for *in situ* MAS NMR under controlled atmosphere in highly symmetrical sealed glass ampoules
- System for registration *in situ* MAS NMR spectra under continuous flow of reagents
- System for compressed inert gas (nitrogen) preparation ensuring MAS NMR experiments in the wide temperature range (from low to high temperatures)



- Setup *in situ* CFMAS NMR conducting experiments with continuous flow of gas-phase reagents through catalyst and simultaneous magic angle spinning [1]

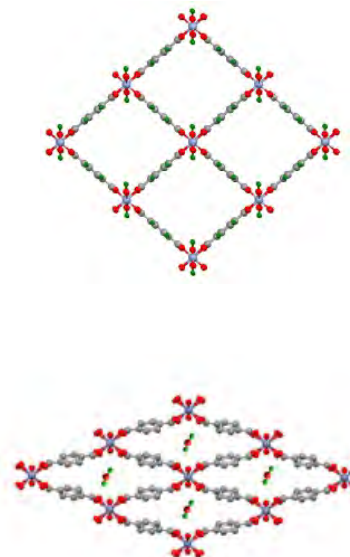
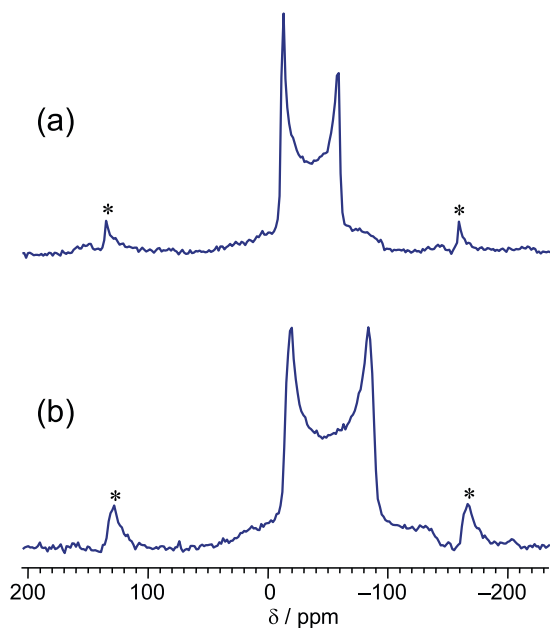
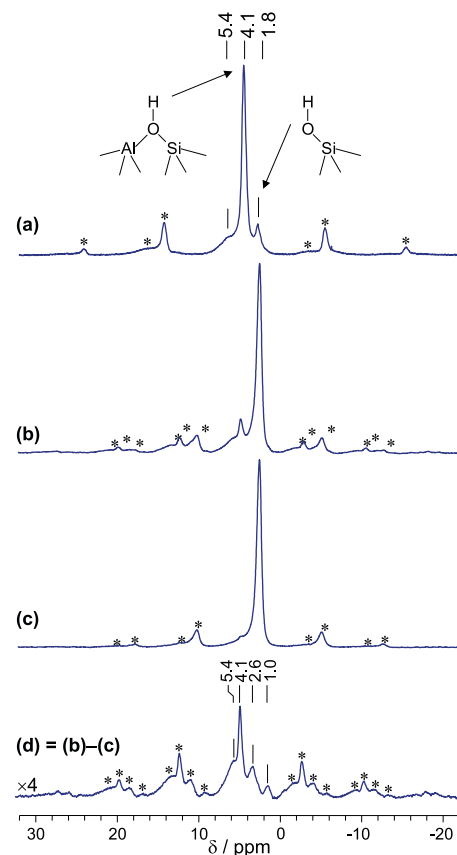


- NMR rotors (4 mm, 7 mm) and sealed glass ampoules prepared for MAS NMR experiments under controlled atmosphere
- Specially designed highly symmetrical ampoules are used (tightly inserted into MAS NMR rotor)
- A sample ( $0.050.20 \text{ cm}^3$ ) is prepared in the special device connected to vacuum system; finally, ampoule with the sample is sealed off thus becoming a mini-reactor for *in situ* MAS NMR experiments
- Vacuum setup allows treatment of the samples under vacuum (or in the specified gaseous atmosphere) and quantitative adsorption of gas/liquid substances on the catalyst

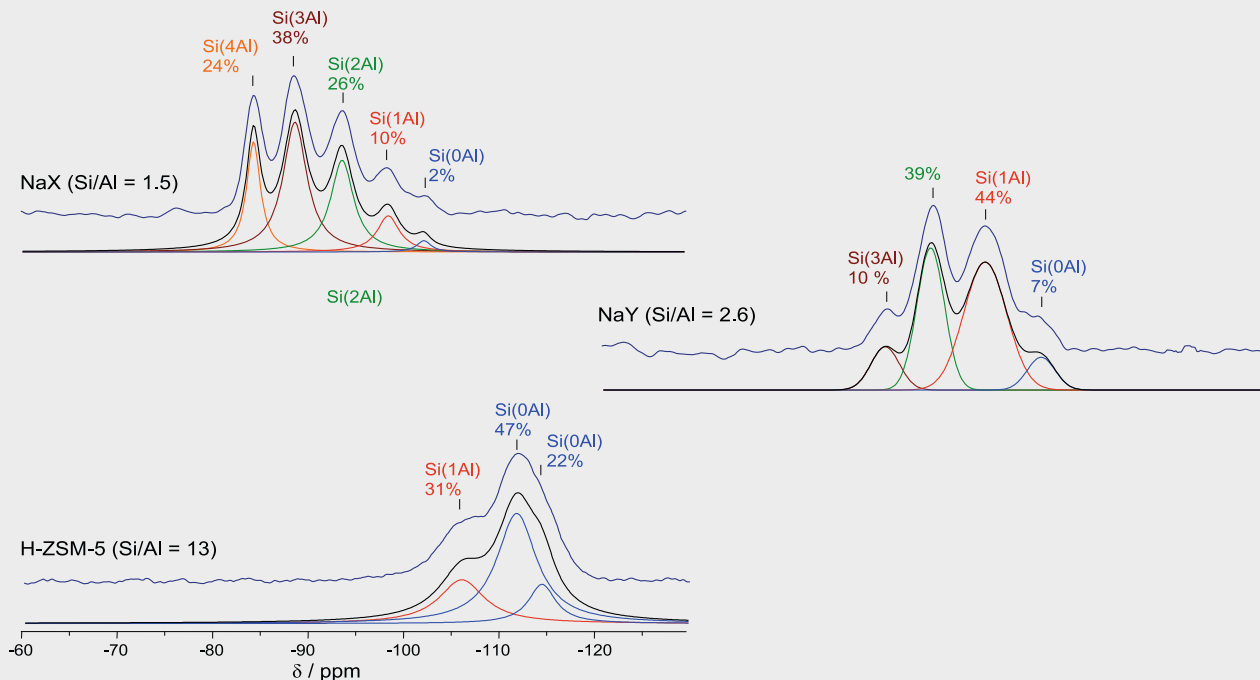


## Capabilities of the techniques applied

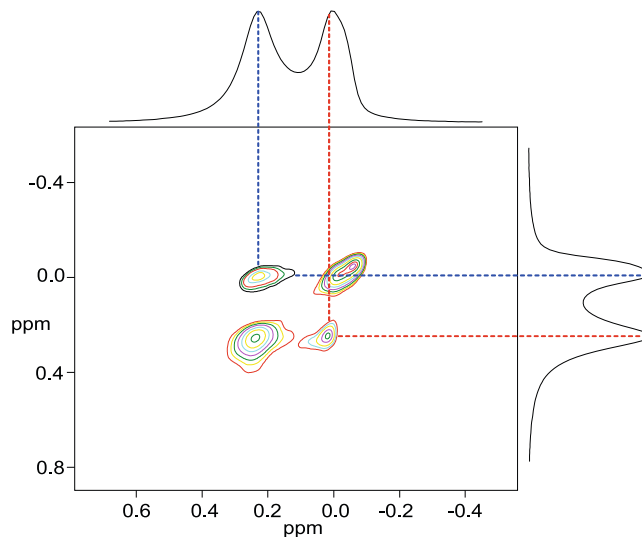
- $^1\text{H}$  MAS NMR method is applied for surface proton sites characterization in zeolite and oxide catalysts and adsorbents. For example, it is possible quantitatively establish distribution of OH-groups of different acidity for zeolites H-ZSM-5 (a) and H-BEA (b)
- $^1\text{H}\{^{27}\text{Al}\}$  MAS NMR TRAPDOR method allows observation of OH groups bound to aluminum atoms (spectra (c) and (d) recorded for zeolite H-BEA) [2]
- $^{27}\text{Al}$  MAS NMR method gives data on structure of zeolite catalysts and metal-organic frameworks, enables to distinguish structural and non-framework aluminum in zeolitic structures and to monitor structural changes in metal-organic frameworks (MOF) induced by different factors. For example,  $^{27}\text{Al}$  MAS NMR spectrum parameters ( $\delta$ ,  $C_Q$ ,  $\eta_Q$ ) are significantly altered when transformation between open (a) and closed (b) structure of metal-organic framework MIL-53(Al) is occurred due to water adsorption



- <sup>29</sup>Si MAS NMR method is applied for zeolite catalysts characterization showing NMR signal with characteristic chemical shift for each type of tetrahedron Si(nAl), n = 0,1,2,3,4, in the zeolite structure. Relation between intensity of different signals gives relative fractions of the Si(nAl) species that allows determination of the ratio Si/Al in different zeolites



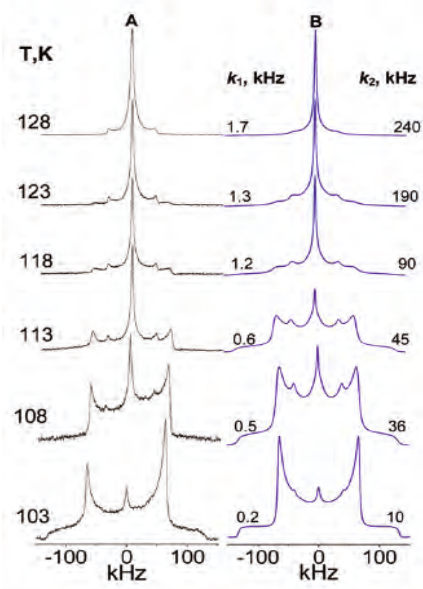
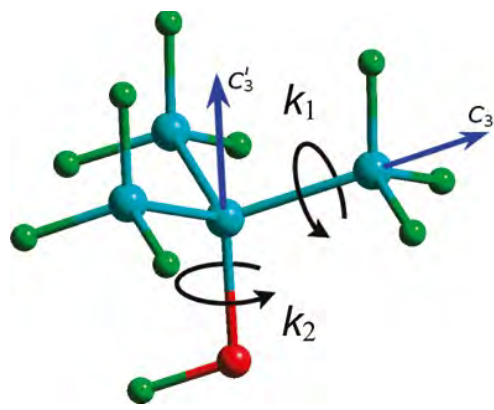
- Two-dimensional exchange <sup>1</sup>H MAS NMR spectroscopy** investigates dynamic equilibrium between gas phase and adsorbed species in zeolites. For example, the presence of cross-peaks in 2D NMR (NOESY) spectrum indicates chemical exchange between methane in the gas phase and in adsorbed state on Zn<sup>2+</sup>/H-ZSM-5 catalyst with characteristic rates of 10 - 60 s<sup>-1</sup> at T = 353 - 363K [3]



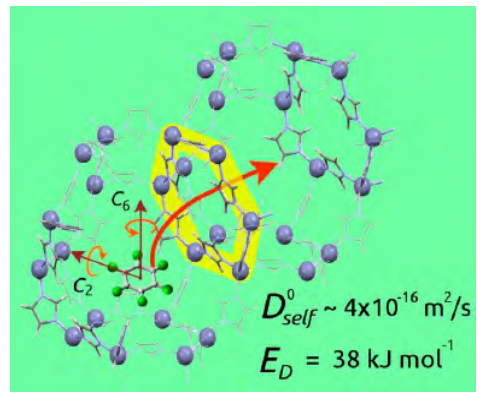
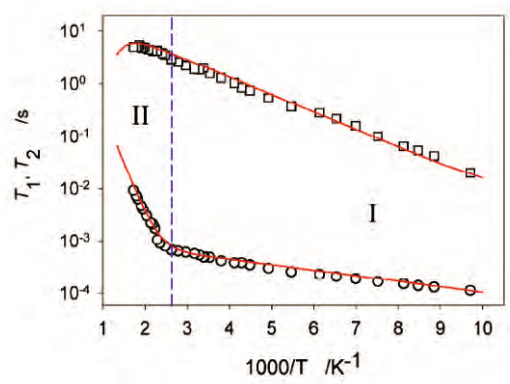
- <sup>2</sup>H NMR spectroscopy for investigation molecular dynamics in micro-mesoporous materials and massive solids. Line shape of solid-state <sup>2</sup>H NMR spectrum is sensitive to geometry of molecular motion. Application of computer modeling allows establishing peculiarities of molecular dynamics with characteristic times  $10 \div 10^3$  s (<sup>2</sup>H NMR stimulated echo),  $10^4 \div 10^7$  s (<sup>2</sup>H NMR solid echo),  $10^6 \div 10^{11}$  s (anisotropic and isotropic T<sub>1</sub>, T<sub>2</sub> spin relaxation)

Objects of research:

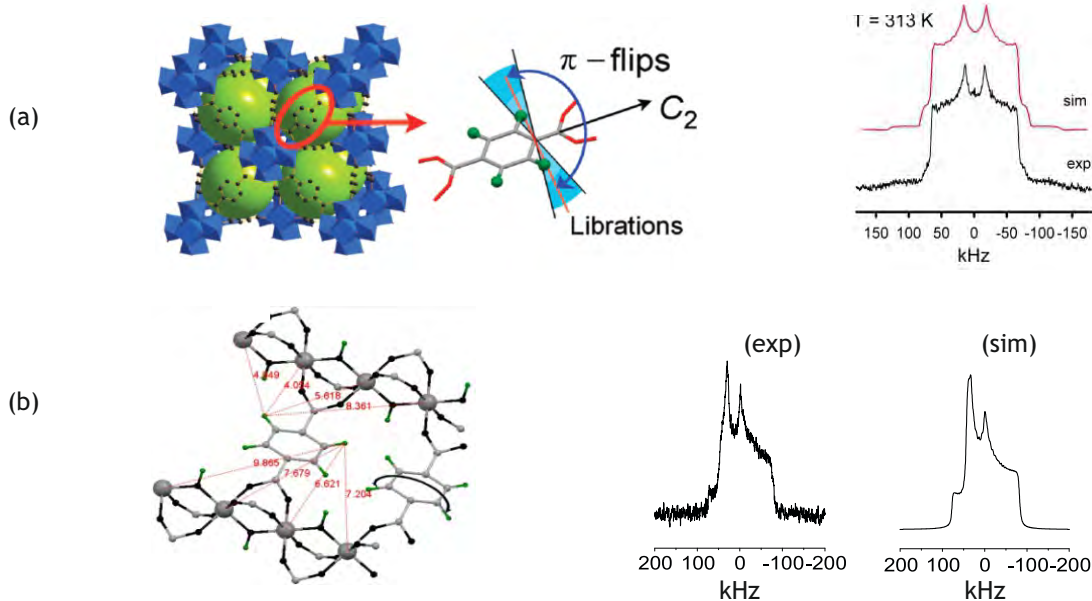
- molecular crystals and crystalline hydrates (tert-butyl alcohol [4], methylimidazole [5], crystalline hydrates CaCl<sub>2</sub>·nH<sub>2</sub>O [6], etc.); for example, from temperature dependence of the line shape in the <sup>2</sup>H NMR spectra it has been established that methyl groups in tert-butyl alcohol rotate about two axes, C<sub>3</sub> and C<sub>3</sub>' [4]



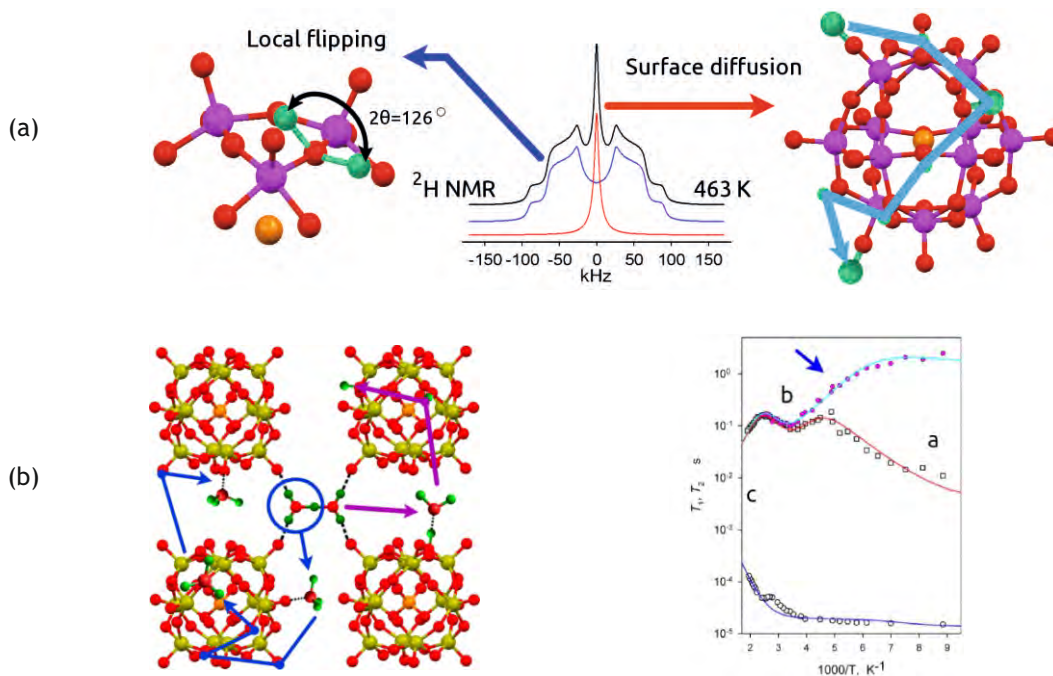
- guest molecules in the porous adsorbents and catalysts of different nature (zeolites, metal-organic frameworks); for example, peculiarities of molecular dynamics of benzene in pores of MOF ZIF-8 have been established on the basis of temperature dependence of spin relaxation [7]



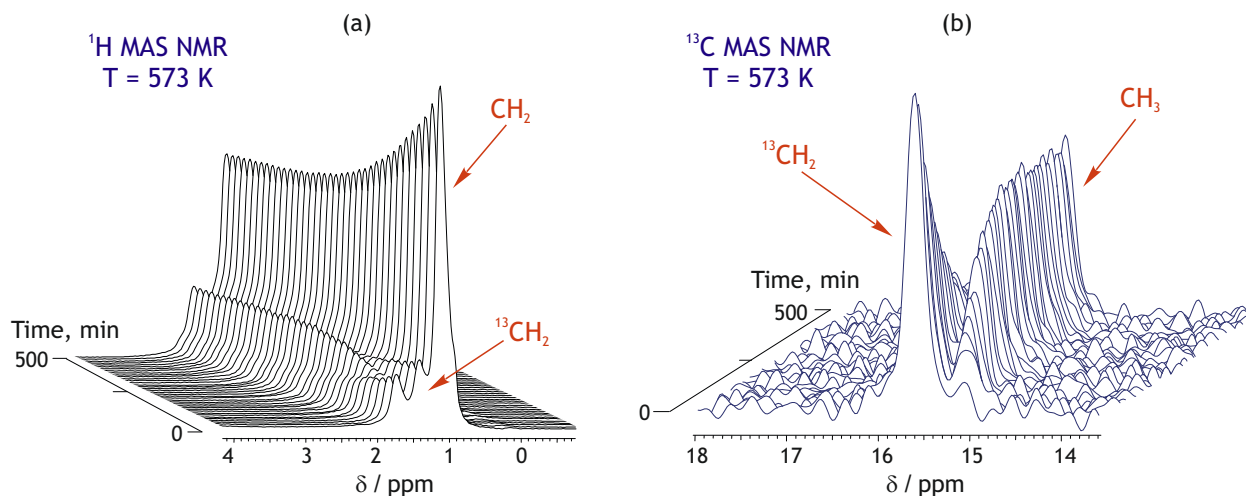
- structural dynamics of different metal-organic frameworks, including those containing diamagnetic cations UiO-66(Zr)[8](a) or paramagnetic cations MIL-53(Cr)[9](b). Data on dynamics for particular fragments of metal-organic frameworks helps to reveal their structure as well as the mechanism of interaction between framework and guest molecules



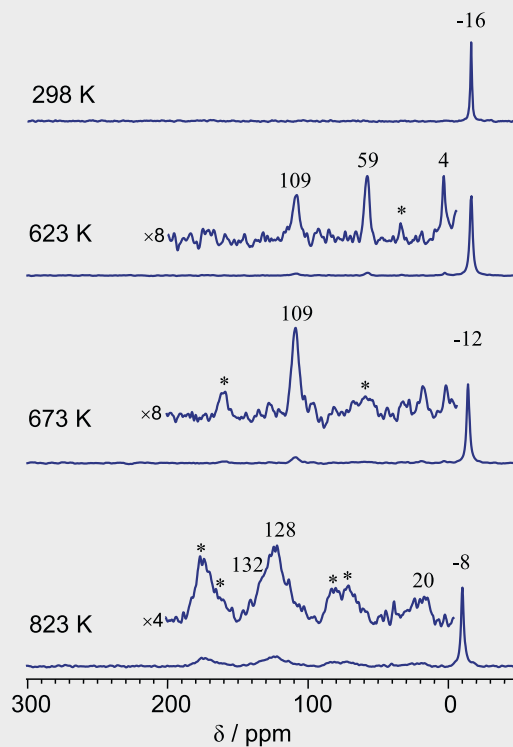
- dynamics of protons in solid acid catalysts, conductivity mechanisms in solid protonic conductors. For example, line shape in the  $^2\text{H}$  NMR spectrum (a)[10] and temperature dependence of relaxation times (b)[11] enable analysis of proton mobility for 12-tungstophosphoric acid



- In situ monitoring of reaction kinetics** is realized by means of sealed NMR ampoules and capability of NMR probe to maintain high temperature (up to 573K) for prolonged times (up to several days [12, 17]). For example, kinetics of  $^{13}\text{C}$  label transfer from  $\text{CH}_2$  group to  $\text{CH}_3$  group in propane molecules adsorbed on zeolite H-ZSM-5 can be analyzed with  $^1\text{H}$  MAS NMR (a)[13] or  $^{13}\text{C}$  MAS NMR (b) [14]



- In situ  $^{13}\text{C}$  CP/MAS NMR method** combining cross-polarization technique and high-power proton decoupling allows identification of intermediates formed in small concentrations on the surface of the catalysts during chemical reaction [15, 16]. Thus, a mechanism of chemical transformation can be established. For example, successive formation of intermediates, methoxy-group (59 ppm), ethane (4 ppm), and ethylene (109 ppm), has been observed during methane transformation into benzene on the surface of  $\text{Ag}^+/\text{H-ZSM-5}$  zeolite [15]



## References

1. Different efficiency of Zn<sup>2+</sup> and ZnO species for methane activation on Zn-modified zeolite. *ACS Catal.* **7** (2017) 1818
2. New insight into the wax precipitation process: *In situ* NMR imaging study in a cold finger cell. *Energy Fuels* **30** (2016) 9003
3. Probing flocculant-induced asphaltene precipitation via NMR imaging: From model toluene - asphaltene systems to natural crude oils. *Appl. Magn. Reson.* **47** (2016) 223
4. Methane interaction with Zn<sup>2+</sup>-exchanged zeolite H-ZSM-5: Study of adsorption and mobility by one- and two-dimensional variable-temperature <sup>1</sup>H solid-state NMR. *J. Phys. Chem. C* **119** (2015) 14255
5. Mobility of the 2-methylimidazolate linkers in ZIF-8 probed by <sup>2</sup>H NMR: Saloon doors for the guests. *J. Phys. Chem. C* **119** (2015) 27512
6. Characterization and dynamics of the different protonic species in hydrated 12-tungstophosphoric acid studied by <sup>2</sup>H NMR. *J. Phys. Chem. C* **118** (2014) 30023
7. Rotational and translational motion of benzene in ZIF-8 Studied by <sup>2</sup>H NMR: Estimation of microscopic self-diffusivity and its comparison with macroscopic measurements. *J. Phys. Chem. C* **118** (2014) 12873
8. Direct <sup>2</sup>H NMR observation of the proton mobility of the acidic sites of anhydrous 12-tungstophosphoric acid. *Chem. Phys. Chem.* **14** (2013) 1783
9. Methane activation and transformation on Ag/H-ZSM-5 zeolite studied with solid-state NMR. *J. Phys. Chem. C* **117** (2013) 7690
10. Probing the dynamics of the porous Zr Terephthalate UiO-66 framework using <sup>2</sup>H NMR and neutron scattering. *J. Phys. Chem. C* **116** (2012) 12131
11. Parahydrogen-induced polarization detected with continuous flow magic angle spinning NMR. *J. Phys. Chem. C* **117** (2013) 2888
12. Mobility of solid tert-butyl alcohol studied by deuterium NMR. *J. Phys. Chem. A* **115** (2011) 7428
13. Dynamics of benzene rings in MIL-53(Cr) and MIL-47(V) frameworks studied by <sup>2</sup>H NMR spectroscopy. *Angew. Chem., Int. Ed.* **49** (2010) 4791
14. Strong acidity of silanol groups of zeolite beta: Evidence from the studies by IR spectroscopy of adsorbed CO and <sup>1</sup>H MAS NMR. *Microporous Mesoporous Mater.* **131** (2010) 210
15. Water dynamics in bulk and dispersed in silica CaCl<sub>2</sub> hydrates studied by <sup>2</sup>H NMR. *J. Phys. Chem. C* **112** (2008) 12853
16. Understanding methane aromatization on a Zn-modified high-silica zeolite. *Angew. Chem. Int. Ed.* **47** (2008) 4559
17. Zn-promoted hydrogen exchange for methane and ethane on Zn/H-BEA zeolite. *In situ* <sup>1</sup>H MAS NMR kinetic study. *J. Catal.* **253** (2008) 11
18. <sup>1</sup>H MAS NMR monitoring of the <sup>13</sup>C-labeled carbon scrambling for propane in zeolite H-ZSM-5. *Chem. Phys. Lett.* **420** (2006) 574
19. *In situ* <sup>1</sup>H and <sup>13</sup>C MAS NMR kinetic study of the mechanism of H/D exchange for propane on zeolite HZSM-5. *J. Phys. Chem. B* **109** (2005) 19748

# Magnetic Resonance

## Electron Spin Resonance (ESR) Spectroscopy

### Scientific and analytical tasks

- The study of physicochemical processes at elevated temperatures and pressures, including sub- and supercritical media, via ESR *in situ*
- The investigation of the formation (including the earliest stages) and evolution of active sites of catalysts based on magnetic nanoparticles or paramagnetic ions via ESR *in situ*
- The investigation of structure and properties of the catalysts and other functional materials using spin probes, labels and spin trapping via ESR including *in situ* regime
- The study of the mechanism of catalytic reactions via registration of active intermediate paramagnetic (radical) species (intermediates)
- The study of the intermolecular interactions and mobility of paramagnetic particles, dynamics of their local environment in different media, including multicomponent hydrocarbon species (heavy oils, asphaltenes, resins etc.) via ESR *in situ*
- Determination of concentration and properties of different types of active sites over oxide catalysts

### Equipment

#### ESR spectrometer Bruker ELEXSYS 500

- Spectra registration in a wide range of temperatures (**77 ÷ 1200 K**) and pressures (up to 300 bar) *in situ* provided by specially designed accessories
- External magnetic field value: **from -17 to 17 kOe**
- High accuracy of the external magnetic field setup:  **$10^{-3}$  Oe** provided by special teslameter E 035M
- **X and Q** modes with **10 and 34 GHz** frequencies of MW irradiation
- High Q-value of the cavities and microwave circuit providing **3000 : 1** “weak” pitch signal to noise ratio. The sensitivity is up to  $10^{10}$  electron spin (1/2) for paramagnetic and  $10^7$  electron spin for ferromagnetic (superparamagnetic) species
- Special mutual geometry of MW and external magnetic fields to study “forbidden” transitions having weak intensity
- Rapid scan regime with **200 Hz** frequency and **200 Oe** amplitude with the possibility of synchronous or direct detection to study fast physicochemical processes
- The single measurement of the signal with the time resolution of **8 nanoseconds** and amplitude of **14 bits**

- The registration of up to five derivatives of the EPR signal; registration of the dispersion signal from conductivity electrons
- Digital automatic goniometer to study orientation behavior of ESR spectra with an angular resolution of **0.125 degree** and a reproducibility of **0.5 degrees**, independent of the direction of rotation



ESR spectrometer Bruker ELEXSYS 500

### The cavities and accessories available

ER 4102ST Standard Resonator: The universal X-Band resonator

ER 5106QT Q-Band Resonators: CW-EPR at 34 GHz

ER 4103TM Cylindrical mode resonator: for aqueous and high-dielectric samples

ER 4104OR Optical transmission resonator: correlate EPR and optical signals

ER 4105DR Double rectangular resonator: quantitative EPR and precise g-factor measurements

ER 4116DM Dual mode resonator: separate allowed and forbidden transitions

ER 4117MX Mixing cell resonator: measure transient paramagnetic species

ER 4122SHQE Super high-Q resonator

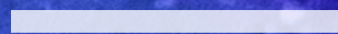
ER 4114HT High temperature resonator: CW-EPR at extreme temperatures

## References

- CO oxidation over Pd/ZrO<sub>2</sub> catalysts: Role of support's donor sites.  
*Molecules* **21** (2016) 1289
- Size effects in the magnetic properties of  $\epsilon$ -Fe<sub>2</sub>O<sub>3</sub> nanoparticles.  
*J. Applied Physics* **118** (2015) 213901
- NMR and EPR spectroscopic identification of intermediates formed upon activation of 8-mesitylimino-5,6,7-trihydroquinolylnickel dichloride with ALR<sub>2</sub>Cl (R = ME, ET).  
*Organomet.* **34** (2015) 3222
- EPR spectroscopic detection of the elusive Fe<sup>V</sup>=O intermediates in selective catalytic oxofunctionalizations of hydrocarbons mediated by biomimetic ferric complexes.  
*ACS Catalysis* **5** (2015) 2702
- In situ* ESR study of molecular dynamics of asphaltenes at elevated temperature and pressure.  
*Energy & Fuels* **28** (2014) 6315
- Size control in the formation of magnetite nanoparticles in the presence of citrate ions.  
*Mater. Chem. Phys.* **145** (2014) 75
- Effect of modification with vanadium or carbon on destructive sorption of halocarbons over nanocrystalline MgO: The role of active sites in initiation of the solid-state reaction.  
*J. Phys. Chem. C* **118** (2014) 13715
- Selective ethylene trimerization by titanium complexes bearing phenoxy-imine ligands: NMR and EPR spectroscopic studies of the reaction intermediates.  
*Organomet.* **33** (2014) 1431
- Surface effects and magnetic ordering in few-nanometer-sized -Fe<sub>2</sub>O<sub>3</sub> particles.  
*J. Appl. Phys.* **114** (2013) 163911
- Hyperfine interactions of narrow-line trityl radical with solvent molecules.  
*J. Magn. Res.* **233** (2013) 29
- Characterization of electron donor sites on Al<sub>2</sub>O<sub>3</sub> surface.  
*Phys. Chem. Chem. Phys.* **14** (2012) 2587
- EPR detection of Fe(V)=O active species in nonheme iron-catalyzed oxidations.  
*Catal. Com.* **29** (2012) 105
- Electron spin resonance of VO<sup>2+</sup> radical-ion in sub- and supercritical water.  
*J. Supercrit. Fluids* **57** (2011) 247
- Characterization of the active sites on the surface of Al<sub>2</sub>O<sub>3</sub> ethanol dehydration catalysts by EPR using spin probes.  
*J. Catal.* **278** (2011) 71
- Characterization of active sites of Pd/Al<sub>2</sub>O<sub>3</sub> model catalysts with low Pd content by luminescence, EPR and ethane hydrogenolysis.  
*Appl. Catal. B* **103** (2011) 397
- EPR spectroscopic trapping of the active species of nonheme iron-catalyzed oxidation.  
*J. Am. Ceram. Soc.* **131** (2009) 10798
- An EPR study of the V(IV) species formed upon activation of a vanadyl phenoxyimine polymerization catalyst with AlR<sub>3</sub> and AlR<sub>2</sub>Cl (R = Me, Et).  
*Macromol. Chem. Phys.* **210** (2009) 542
- Ferromagnetic resonance study of thin film antidot arrays: Experiment and micromagnetic simulations.  
*Phys. Rev. B* **75** (2007) 174429
- FMR fine structure - a tool to investigate the spatial magnetic phase separation phenomena in manganites.  
*Physica Status Solidi-Rapid Research Letters* **1** (2007) R22-R24.
- EPR identification of Zr(III) complexes formed upon interaction of (2-PhInd)<sub>2</sub>ZrCl<sub>2</sub> and *rac*-Me<sub>2</sub>Si(1-Ind)<sub>2</sub>ZrCl<sub>2</sub> with MAO and MMAO.  
*Macromol. Chem. Phys.* **208** (2007) 1168
- Ferromagnetic resonance investigation of collective phenomena in two-dimensional periodic arrays of Co particles.  
*Appl. Phys. A: Mater. Sci. & Process.* **81** (2005) 679
- Manifestation of granular structure in FMR spectra.  
*J. Magn. Magn. Materials* **267** (2003) 13
- EPR and <sup>1</sup>H NMR spectroscopic study of the Cr<sup>III</sup>(salen) Cl catalysts.  
*J. Chem. Soc. - Dalton Trans.* **11** (2002) 2263
- <sup>1</sup>H NMR and EPR spectroscopic monitoring of the reactive intermediates of (Salen) Mn<sup>III</sup> catalyzed olefin epoxidation.  
*J. Mol. Catal. A - Chem.* **158** (2000) 19

The mixture of rare earth elements oxides

X10,000



1μm

# Fourier-Transformed Infrared Spectroscopy (FT-IR)

## Fourier-Transformed Infrared Spectroscopy (FT-IR)

### Scientific and analytical tasks

- *In situ* study of the kinetics and mechanisms of heterogeneous catalytic reactions including analysis of the gas phase
- *Ex situ* analysis of molecular structure of gases, liquids, and solids
- The study of the structure of molecular and ionic crystals

### Equipment

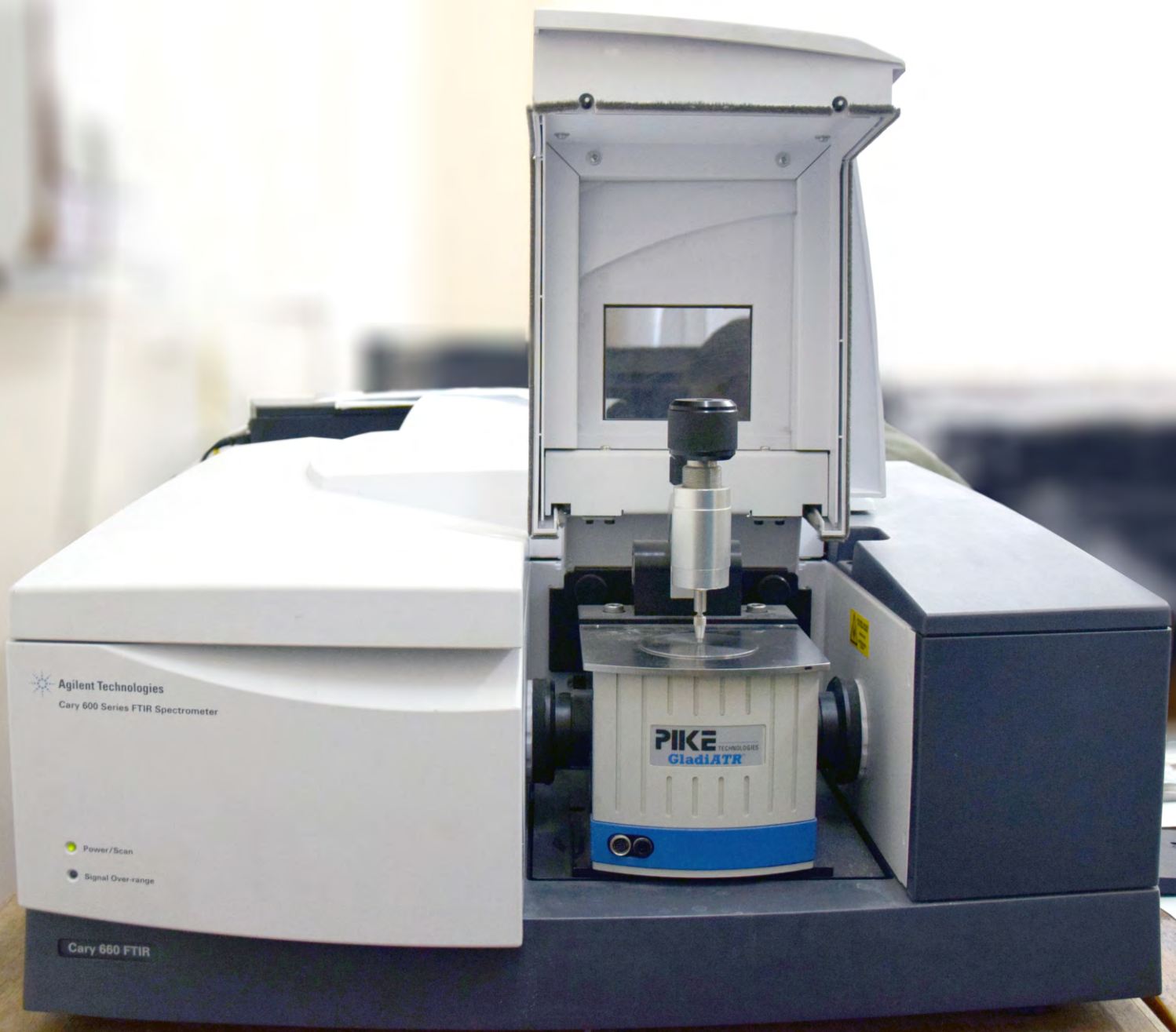
- FT-IR spectrometer Cary 660 (Agilent Technologies)
- Attenuated Total Reflection (ATR) accessory GladiATR (PIKE Technologies)

### *In situ measurements*

- Transmittance regime of spectral measurement
- Spectral range: 4000 - 1000  $\text{cm}^{-1}$
- Spectral resolution: 4  $\text{cm}^{-1}$
- Number of scans: 5 - 40
- Cell volume: 1.5 ml
- Flow rate: 50 - 300 ml/min
- Sample wafers: 1 cm  $\times$  3 cm, 30 - 70 mg
- Activation condition: 200 - 300  $^{\circ}\text{C}$ , air flow
- Temperature of experiments: 20 - 400  $^{\circ}\text{C}$

### *Ex situ measurements*

- Transmittance and ATR regimes of spectral measurement
- Spectral range: 14000 - 250  $\text{cm}^{-1}$
- Spectral resolution:  $\geq 0.5 \text{ cm}^{-1}$
- Scanning rate: 1 scan/sec at spectral resolution of 4  $\text{cm}^{-1}$



FT-IR spectrometer Cary 660  
(Agilent Technologies)

# Fourier-Transformed Infrared Spectroscopy (FT-IR)

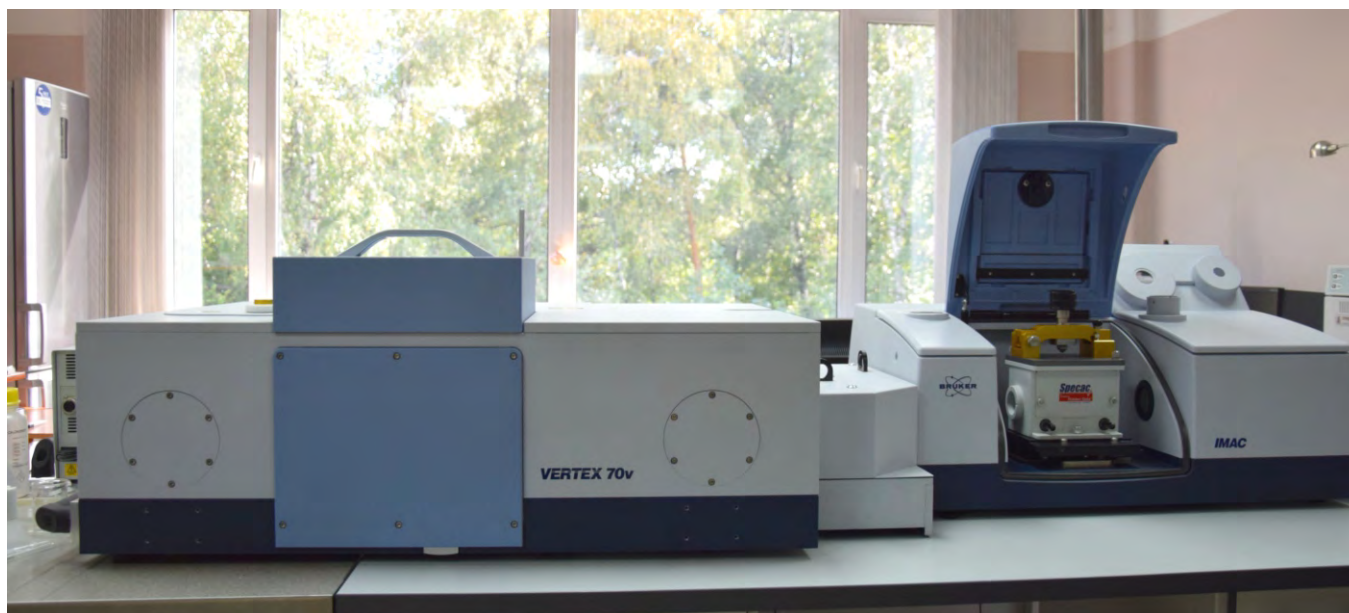
## Fourier-Transformed Infrared Spectroscopy in Supercritical Fluids (SCF) *In Situ*

### Scientific and analytical tasks

- Study of molecular structure of gases, liquids, and solids Including at high temperature and high pressure
- Obtaining of FT-IR images of polymers, mixtures, composites and biological tissues in addition study of dynamic systems, such as dissolution, diffusion, microfluidics, etc.
- *In situ* study of samples, sorption processes and catalytic reactions at supercritical fluid temperature and pressure condition also in the FT-IR imaging regime

### Equipment

- FT-IR spectrometer VERTEX 70v (Bruker) equipped with DLaTGS and MCT detectors
- Attenuated Total Reflection (ATR) accessory High Temperature Golden Gate ATR and Super Critical Fluids Golden Gate ATR (Specac)
- IMAC imaging macro chamber (Bruker) equipped with a focal plane array (FPA) detector with 64 x 64 pixels [a multi-channel mercury cadmium telluride (MCT) detector] and Imaging Golden Gate diamond ATR accessory (Specac)



## *In situ* measurements

- ATR regime of spectral measurement
- Spectral range: 5000 - 500  $\text{cm}^{-1}$
- Spectral resolution:  $\geq 0,4 \text{ cm}^{-1}$
- Cell volume: 28  $\mu\text{l}$
- Flow rate: 0.1 - 100 ml/min
- Temperature of experiments: 20 - 300  $^{\circ}\text{C}$
- Pressure: up to 400 atm (6000 p.s.i.)

## *FT-IR imaging* measurements

- Transmittance and ATR regime of spectral measurement
- Spectral resolution: 4  $\text{cm}^{-1}$
- Lateral resolution: 10 - 15  $\mu\text{m}$  (ATR)
- Spectral range: 3800 - 900  $\text{cm}^{-1}$
- Field of View (FOV)/image: 625  $\times$  625  $\mu\text{m}$  (ATR)



## References

1. Redox mechanism for selective oxidation of ethanol over monolayer  $\text{V}_2\text{O}_5/\text{TiO}_2$  catalysts.  
*J. Catal.* **338** (2016)
2. Behavior of asphaltenes in crude oil at high-pressure  $\text{CO}_2$  conditions: An *in situ* ATR-FTIR spectroscopic imaging study.  
*Energy Fuels* **30** (2016) 4750
3. Effect of temperature and composition on the stability of crude oil blends studied with chemical imaging *in situ*.  
*Energy Fuels* **29** (2015) 7114
4. Chemical visualization of asphaltenes aggregation processes studied *in situ* with ATR-FTIR spectroscopic imaging and NMR imaging.  
*J. Phys. Chem. C* **119** (2015) 2646
5. Propane ammoxidation on Bi promoted  $\text{MoVTeNbO}_x$  oxide catalysts: Effect of reaction mixture composition.  
*Appl. Catal. A* **506** (2015) 109
6. Selective dehydrogenation of propane to propene with  $\text{O}_2\text{-H}_2$  on bifunctional  $\text{Pt-H}_3\text{PMo}_{12}\text{O}_{40}$  catalysts.  
*Appl. Catal. A* **477** (2014) 1
7. Doping magnesium hydroxide with sodium nitrate: A new approach to tune the dehydration reactivity of heat-storage materials.  
*ACS Appl. Mater. Interfaces* **6** (2014) 19966
8. Selective oxidation of methanol to form dimethoxymethane and methyl formate over a monolayer  $\text{V}_2\text{O}_5/\text{TiO}_2$  catalyst.  
*J. Catal.* **311** (2014) 59
9. FTIR study of  $\beta$ -picoline and pyridine-3-carbaldehyde transformation on V-Ti-O catalysts. The effect of sulfate content on  $\beta$ -picoline oxidation into nicotinic acid.  
*J. Molec. Catal. A* **380** (2013) 118
10. FTIR study of the surface complexes of  $\beta$ -picoline, 3-pyridine-carbaldehyde and nicotinic acid on sulfated  $\text{TiO}_2$  (anatase).  
*J. Molec. Catal. A* **373** (2013) 96
11. Structure and properties of tungsten peroxopolyoxo complexes - promising catalysts for organics oxidation. II: Cation type influence on the tungsten peroxocomplex structure.  
*J. Molec. Catal. A* **366** (2013) 341
12. Effect of water on decomposition of formic acid over V-Ti oxide catalyst: Kinetic and *in situ* FTIR study.  
*J. Molec. Catal. A* **357** (2012) 148
13. Mechanism of the oxygen involvement in nicotinic acid formation under  $\beta$ -picoline oxidation on V-Ti-O catalyst.  
*Catal. Today* **157** (2010) 39
14. Hybrid polyoxotungstate/MIL-101 materials: Synthesis, characterization, and catalysis of  $\text{H}_2\text{O}_2$ -based alkene epoxidation.  
*Inorg. Chem.* **49** (2010) 2920
15. Structure and electrical conductivity of nitrogen-doped carbon nanofibers.  
*Carbon* **47** (2009) 1922.
16. Heterogeneous selective oxidation catalysts based on coordination polymer MIL-101 and transition metal-substituted polyoxometalates.  
*J. Catal.* **257** (2008) 315
17. Heterogeneous selective oxidation of formaldehyde to formic acid on V/Ti oxide catalysts: The role of vanadia species.  
*J. Molec. Catal. A* **283** (2008) 146
18. Aerobic oxidations of  $\alpha$ -pinene over cobalt-substituted polyoxometalate supported on amino-modified mesoporous silicates.  
*J. Catal.* **246** (2007) 241

# Fourier-Transformed Infrared Spectroscopy (FT-IR)

## Wide Temperature FT-IR Spectroscopy of Adsorbed Molecules Using Transmission, Diffusion Reflection, and Attenuated Total Reflection (ATR) Technique

### Scientific and analytical tasks

- Quantity measurements of acid-base properties of catalyst surface
- *In situ* study of mechanisms of heterogeneous catalytic reactions

### Equipment

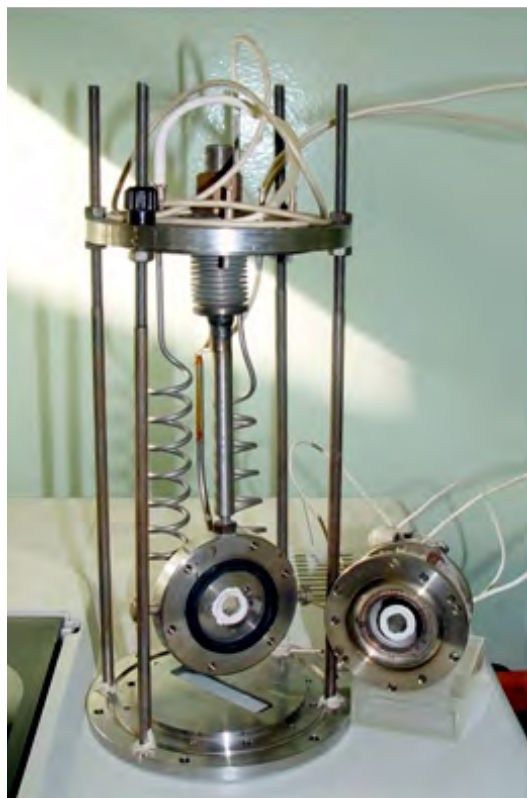
The available FTIR spectrometers are characterized by a resolution of 1 to 16  $\text{cm}^{-1}$  in the range of 5000 - 350  $\text{cm}^{-1}$ : **Shimadzu FT-IR 8300, 8400, and IR prestige**. The methods of acid-base measurement are unique and allow quantitative measuring of the strength and concentration of Lewis and Brønsted acid, as well as the basic sites. The minimum concentration of sites can be measured at the level of 0.05  $\mu\text{mol/g}$ .

*In situ* study of catalytic reaction mechanisms at temperatures 77 - 773 K



### References

1. Sol-gel synthesis of mesoporous aluminosilicates with a narrow pore size distribution and catalytic activity thereof in the oligomerization of dec-1-ene.  
*Microporous Mesoporous Mater.* **230** (2016) 118
2. Hydroprocessing of hydrocracker bottom on Pd containing bifunctional catalysts.  
*Catal. Today* **271** (2016) 154
3. Influence of boron addition to alumina support by kneading on morphology and activity of HDS catalysts.  
*Appl. Catal. B* **199** (2016) 23
4. Effect of impregnation on the structure of niobium oxide/alumina catalysts studied by multinuclear solid-state NMR, FTIR, and quantum chemical calculations.  
*J. Phys. Chem. C* **119** (2015) 10400
5. Strong acidity of silanol groups of zeolite beta: Evidence from the studies by IR spectroscopy of adsorbed CO and  $^1\text{H}$  MAS NMR.  
*Microporous Mesoporous Mater.* **131** (2010) 210
6. Synthesis and characterization of mesoporous silica thin films as a catalyst support on a titanium substrate.  
*Thin Solid Films* **515** (2007) 6391
7. Nanostructured, Gd-doped ceria promoted by Pt or Pd: Investigation of the electronic and surface structures and relations to chemical properties.  
*J. Phys. Chem. B* **109** (2005) 20077



Homemade high-temperature flow IR cell with gas pathway 0.5 mm for a temperature range of 25 - 400 °C



High-temperature flow IR cell with gas pathway 5 mm in sample chamber of spectrometer IR-Prestige (Shimadzu) for a temperature range of 25 - 400 °C



Wide temperature IR cell  
Working temperature range is 77 - 773 K

# Raman Spectroscopy

## Scientific and analytical tasks

- The study of the structure of oxide and sulfide catalysts, including supported and bulk materials
- The study of the structure of molecular and ionic crystals
- The study of the structure of some complex compounds in aqueous and non-aqueous solutions

## Equipment

### Fourier-Raman spectrometer Bruker RFS-100/S

- 1064 nm line of Nd-YAG laser as source of Raman effect
- Power: 0 - 500 mW
- Laser spot: 50  $\mu\text{m}$
- InGaAs detector
- Raman scattering geometry: 90 and 180°
- Spectral resolution:  $\geq 0.5 \text{ cm}^{-1}$
- Spectral range: 100 - 3700  $\text{cm}^{-1}$



## References

1. Doping magnesium hydroxide with sodium nitrate: A new approach to tune the dehydration reactivity of heat-storage materials. *ACS Appl. Mater. Interfaces* **6** (2014) 19966.
2. FTIR study of  $\beta$ -picoline and pyridine-3-carbaldehyde transformation on V-Ti-O catalysts. The effect of sulfate content on  $\beta$ -picoline oxidation into nicotinic acid. *J. Molec. Catal. A* **380** (2013) 118.
3. FTIR study of the surface complexes of  $\beta$ -picoline, 3-pyridine-carbaldehyde and nicotinic acid on sulfated  $\text{TiO}_2$  (anatase). *J. Molec. Catal. A* **373** (2013) 96.
4. Vibrational spectra of  $\text{WO}_3 \cdot n\text{H}_2\text{O}$  and  $\text{WO}_3$  polymorphs. *Vibr. Spectrosc.* **55** (2011) 235.
5. Iron tetrasulfophthalocyanine immobilized on metal organic framework MIL-101: Synthesis, characterization and catalytic properties. *Dalton Trans.* **40** (2011) 1441.
6. High-active hydrotreating catalysts for heavy petroleum feeds: Intentional synthesis of CoMo sulfide particles with optimal localization on the support surface. *Catal. Today* **150** (2010) 164.
7. Highly selective oxidation of alkylphenols to benzoquinones with hydrogen peroxide over silica-supported titanium catalysts: Titanium cluster site versus titanium single site. *Adv. Synth. Catal.* **351** (2009) 1877.
8. Structure and electrical conductivity of nitrogen-doped carbon nanofibers. *Carbon* **47** (2009) 1922.
9. The state of absorbed hydrogen in the structure of reduced copper chromite from the vibration spectra. *Phys. Chem. Chem. Phys.* **11** (2009) 6090.
10. The investigation of chemical and phase composition of solid precursor of MoVTenb oxide catalyst and its transformation during the thermal treatment. *Appl. Catal. A* **353** (2009) 249.
11. Formation of active phases in MoVTenb oxide catalysts for ammoxidation of propane. *Catal. Today* **144** (2009) 312.
12. FT-IR and FT-Raman spectra of five polymorphs of chlorpropamide. Experimental study and ab initio calculations. *J. Molec. Struct.* **891** (2008) 75.

# Ultraviolet-Visible (UV-Vis) Spectroscopy

## Ultraviolet-Visible Diffuse Reflectance Spectroscopy (UV-Vis DRS)

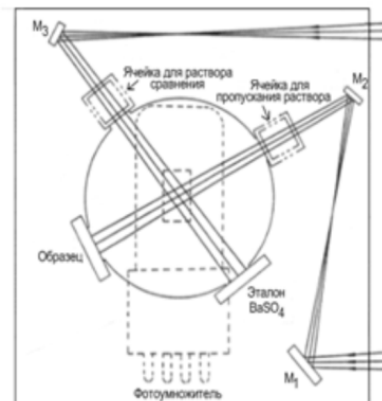
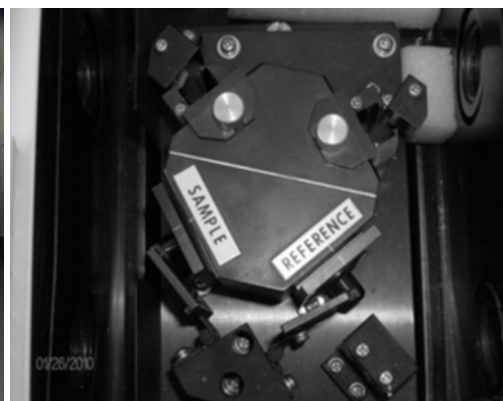
### Scientific and analytical tasks

- *In situ* study of the formation and evolution of active species of homogeneous catalysts
- The study of homogeneous and heterogeneous catalytic reactions
- The determination of the content of d-metals in solutions using the transmission spectra of their colored complexes
- The determination of the structure of impurity sites on the surface and in the bulk of support (oxidation state, coordination number, nature of the ligand), establishing the structure, particle size, band gap of semiconductors and dielectrics
- The investigation of the electronic state (the coordination number, ligand environment, band gap) of cations of d-metals stabilized in oxide and zeolite matrix to identify the catalytically active states (isolated ions, associated ions, oxide clusters, oxide nanoparticles) of heterogeneous catalysts
- The study of optical properties of Cu, Ag, and Au nanosized particles in heterogeneous catalysts and colloidal solutions using plasmon resonance spectra
- The study of band gap of catalysts based on semiconductor oxides (TiO<sub>2</sub>, CeO<sub>2</sub>, SiO<sub>2</sub>, CuO, etc.)
- The study of changes (genesis) in the electronic state (valence state, coordination number, band gap) of cations of d-metals and semiconductors in heterogeneous catalysts caused by structural and structural-phase and polymorphic transformations, processes of hydration and dehydration, reactions of oxidation and reduction as a result of influence of different reaction media and temperature

### Equipment

- **Shimadzu UV-2501 PC spectrophotometer with ISR-240A diffuse reflectance unit**
  - Wavelength range: 190 - 900 nm (performance guaranteed range)
  - Monochromator system: Double monochromator with a high-performance double-blazed holographic grating in the aberration corrected Czerny-Turner mounting
  - Resolution: 0.1 nm
  - Spectral bandwidth: 0.1, 0.2, 0.5, 1, 2 and 5 nm
  - Wavelength repeatability: ±0.1 nm
  - Wavelength accuracy: ±0.3 nm
  - Photometric mode: Absorbance (Abs.), transmittance (%), reflectance (%) and energy (E)
  - Photometric range: Absorbance: -4-5 Abs. (0.001 Abs. increments)

- Transmittance: 0 - 999.9 % (0.01% increments)
- Reflectance: 0 - 999.9 % (0.01% increments)
- Photometric accuracy:  $\pm 0.002$  Abs. (0 - 0.5 Abs.);  $\pm 0.004$  Abs. (0.5 - 1 Abs.)
- Photometric repeatability:  $\pm 0.001$  Abs. (0 - 1.0 Abs.)  $\pm 0.1$  %T
- Baseline flatness: Within  $\pm 0.001$  Abs. (excluding noise; 2 nm slit width and slow wavelength scanning speed)
- Drift: Less than 0.0004 Abs. per hour (after 2 hours warm-up)

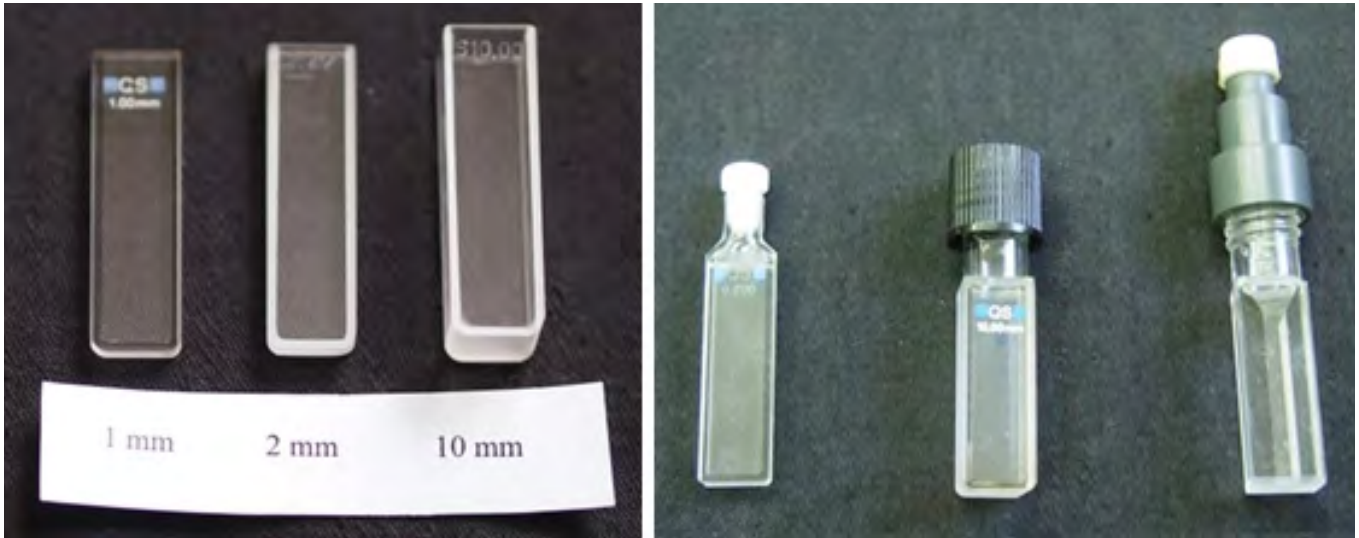


- **ISR-240A Integrating Sphere Attachment, 60 mm dia (P/N206-23860-91)**

This attachment is used for measurement of diffuse and total reflectance and measurement of transmission of liquid or solid sample:

- Wavelength range: 220 - 800 nm
- Integrating sphere: 60 mm in inner diameter, equipped with a photomultiplier
- Maximum size of reflection sample: 40 × 70 mm wide, 10 mm thick or 70 × 70 mm wide, 5 mm thick
- Incident angle: 90 deg

### Optical cells for *ex situ* studies of powders and solutions



### Flow optical cells for *in situ* studies of powders



## References

1. The role of chemisorbed water in formation and stabilization of active sites on Pd/Alumina oxidation catalysts.  
*Catal. Today* (2017) DOI: 10.1016/j.cattod.2017.01.033
2. Novel photocatalysts Pt/Cd<sub>1-x</sub>Zn<sub>x</sub>S/ZnO/Zn(OH)<sub>2</sub>: Activation during hydrogen evolution from aqueous solutions of ethanol under visible light.  
*Appl. Catal. B* **183** (2016) 197
3. Hydroprocessing of hydrocracker bottom on Pd containing bifunctional catalysts.  
*Catal. Today* **271** (2016) 154
4. Effect of metal-metal and metal-support interaction on activity and stability of Pd Rh/Alumina in CO oxidation.  
*Catal. Today* (2016) DOI: 10.1016/j.cattod.2016.10.010
5. Cu-substituted ZSM-5 catalyst: Controlling of DeNOx reactivity via ion-exchange mode with copper-ammonia solution.  
*Appl. Catal. B* **170-171** (2015) 241
6. Synthesis and solar light catalytic properties of titania-cadmium sulfide hybrid nanostructures.  
*Catal. Commun.* **68** (2015) 61
7. Photogeneration of hydrogen from water starting from hybrid Mo<sub>3</sub>S<sub>7</sub> clusters immobilized over TiO<sub>2</sub>.  
*Chem. Sus. Chem.* **8** (2015) 148
8. Effect of titania regular macroporosity on the photocatalytic hydrogen evolution on Cd<sub>1-x</sub>Zn<sub>x</sub>S/TiO<sub>2</sub> catalysts under visible light.  
*Chem. Cat. Chem.* **7** (2015) 4108
9. Photocatalytic hydrogen evolution from aqueous solutions of Na<sub>2</sub>S/Na<sub>2</sub>SO<sub>3</sub> under visible light irradiation on CuS/Cd<sub>0.3</sub>Zn<sub>0.7</sub>S and Ni<sub>2</sub>Cd<sub>0.3</sub>Zn<sub>0.7</sub>S<sub>1-z</sub>.  
*Chem. Eng. J.* **262** (2015) 146
10. Zirconium allyl complexes as participants in zirconocene-catalyzed  $\alpha$ -olefin polymerizations.  
*Ang. Chem. Int. Ed.* **53** (2014) 9645
11. Stabilization of active sites in alloyed Pd-Rh catalysts on  $\gamma$ -Al<sub>2</sub>O<sub>3</sub> support.  
*Catalysis Today* **238** (2014) 80
12. UV-Vis DRS study of valeric acid ketonization mechanism over ZrO<sub>2</sub> in hydrogen atmosphere.  
*J. Molec. Catal. A* **388-389** (2014) 133
13. Selective oxidation of formaldehyde to formic acid over supported vanadia catalysts.  
*Appl. Catal. A* **475** (2014) 98
14. Photocatalytic oxidation of ethanol and isopropanol vapors on cadmium sulfide.  
*J. Catal.* **287** (2012) 138
15. Regulation of the copper-oxide cluster structure and DeNOx activity of Cu-ZSM-5 catalysts by variation of OH/Cu<sup>2+</sup>.  
*Catal. Today* **197** (2012) 214
16. Characterization of active sites of Pd/Al<sub>2</sub>O<sub>3</sub> model catalysts with low Pd content by luminescence, EPR and ethane hydrogenolysis.  
*Appl. Catal. B* **103** (2011) 397
17. Iron tetrasulfophthalocyanine immobilized on metal organic framework MIL-101: Synthesis, characterization and catalytic properties.  
*Dalton Trans.* **40** (2011) 1441
18. Metal-support interactions in Pt/Al<sub>2</sub>O<sub>3</sub> and Pd/Al<sub>2</sub>O<sub>3</sub> catalysts for CO oxidation.  
*Appl. Catal. B* **97** (2010) 57
19. Clean catalytic oxidation of 8-hydroxyquinoline to quinoline-5,8-dione with tBuOOH in the presence of covalently bound FePcS-SiO<sub>2</sub> catalysts.  
*Green Chem.* **12** (2010) 1076
20. Characterization of Rh/Al<sub>2</sub>O<sub>3</sub> catalysts after calcination at high temperatures under oxidizing conditions by luminescence spectroscopy and catalytic hydrogenolysis.  
*Appl. Catal. B* **90** (2009) 141

# Ultraviolet-Visible (UV-Vis) Spectroscopy

## Photoluminescence Spectroscopy

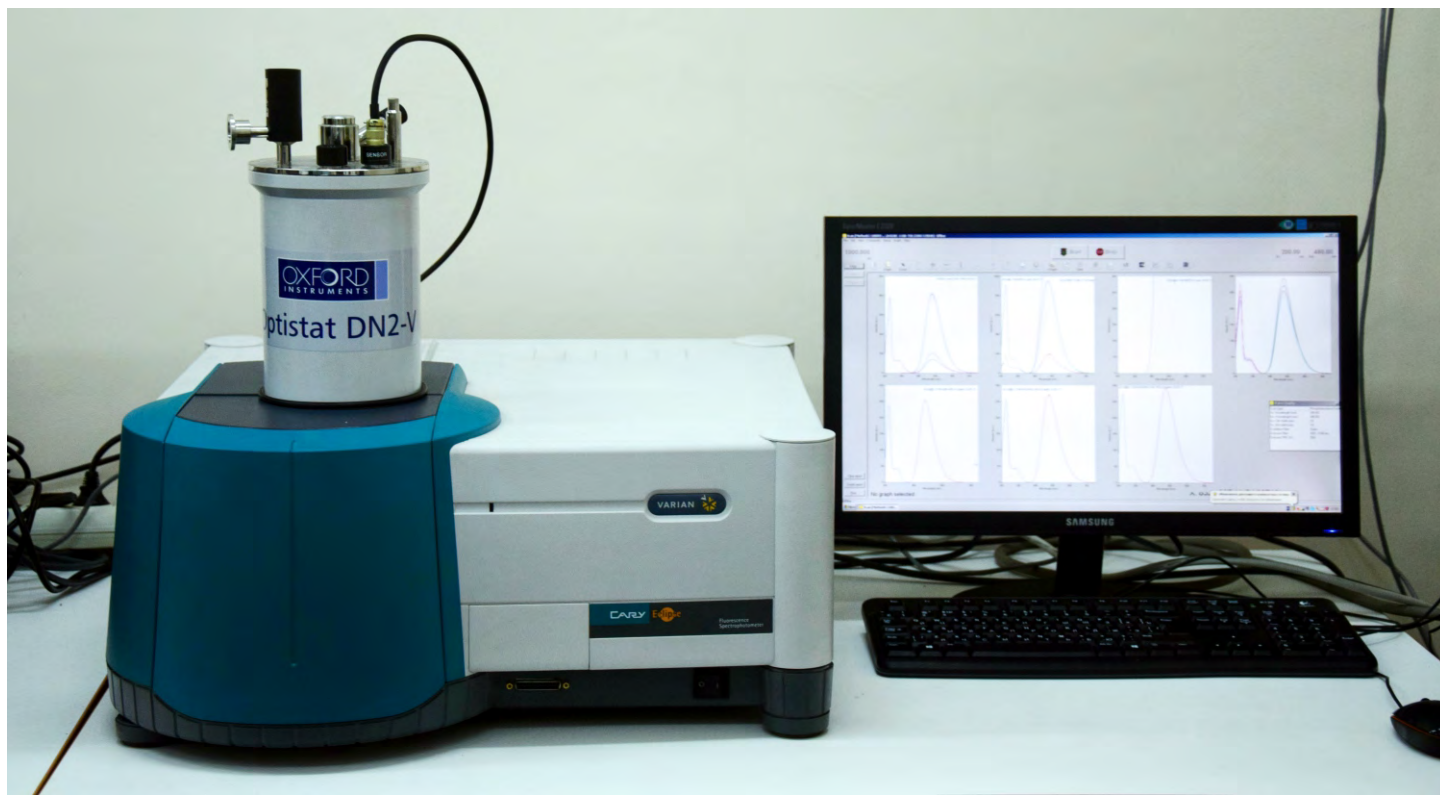
### Scientific and analytical tasks

- Investigation of the structure of liquids and solids by fluorescent probes (molecules, ions of impurity and intrinsic defects for oxides)
- Identification of substances: the high sensitivity of the method can be used for detecting small concentrations. For substances with a quantum yield  $F > 0.5$  the detection limit is about pmol/L

### Equipment

#### Spectrofluorimeter Cary Eclipse Agilent

- 2 super-fast scanning monochromators
- Wavelength range: 200 - 900 nm
- Fluorescence, phosphorescence, chemi- and bioluminescence measurement modes
- For measurements in the temperature range 77 - 500K at vacuum conditions fluorescence spectrophotometer equipped with cryostat Optistat<sup>®</sup>DN-V (Oxford Instruments, UK) with an oil-free Turbopumping system TS75D2001 (EDWARDS)
- Light source: Xenon flash lamp
- The pulse frequency: 80 Hz
- The pulse width at half maximum: 2 ms, the peak power: 75 kW
- Monochromators: Czerny-Turner 0.125 m
- The spectral width of the slit:  
Excitation: 1.5, 2.5, 5, 10, 20 nm and 10 nm round  
Emission: 1.5, 2.5, 5, 10, 20 nm and 10 nm round
- Spectral accuracy:  $\pm 1.5$  nm
- Reproducibility of wavelength:  $\pm 0.2$  nm
- Scan speed: 0.01 - 24 000 nm/min
- Averaging the signal:  
Fluorescence with 0.0125 - 999 s  
Phosphorescence of 1 ms - 10 s
- Bio- and chemiluminescence: 40 ms - 10 s
- Sensitivity: 0.48 pM for fluorescein in 0.01 M NaOH
- 20 nM benzopyrene
- Accuracy of the cryostat temperature range: 77 - 500 K -  $\pm 0.1$  K



Spectrofluorimeter  
Cary Eclipse Agilent

## References

1. The role of chemisorbed water in formation and stabilization of active sites on Pd/Alumina oxidation catalysts. *Catal. Today* (2017) DOI: 10.1016/j.cattod.2017.01.033
2. Effect of alumina phase transformation on stability of low-loaded Pd-Rh catalysts for CO oxidation. *Top. Catal.* (2016) DOI: 10.1007/s11244-016-0726-4
3. Effect of metal-metal and metal-support interaction on activity and stability of Pd Rh/Alumina in CO oxidation. *Top. Catal.* (2016) DOI: 10.1016/j.cattod.2016.10.010
4. Design of functionally graded multilayer thermal barrier coatings for gas turbine application. *Surface & Coatings Technology* **295** (2016) 20
5. Stabilization of active sites in alloyed Pd-Rh catalysts on  $\gamma$ -Al<sub>2</sub>O<sub>3</sub> support. *Catal. Today* **238** (2014) 80
6. Catalytic purification of exhaust gases over Pd-Rh alloy catalysts. *Top. Catal.* **56** (2013) 1008
7. Optical spectroscopy of Pr<sup>3+</sup>-doped  $\gamma$ -BiB<sub>3</sub>O<sub>6</sub> crystals. *Opt. Mater.* **36** (2013) 509
8. Characterization of active sites of Pd/Al<sub>2</sub>O<sub>3</sub> model catalysts with low Pd content by luminescence, EPR and ethane hydrogenolysis. *Appl. Catal., B: Environmental* **103** (2011) 397
9. Characterization of Rh/Al<sub>2</sub>O<sub>3</sub> catalysts after calcination at high temperatures under oxidizing conditions by luminescence spectroscopy and catalytic hydrogenolysis. *Appl. Catal., B: Environmental* **90** (2009) 141

# Elemental Analysis

## X-Ray Fluorescence (XRF)

### Scientific and analytical tasks

Non-destructive analytical method suitable for quantitative and semi-quantitative elemental analysis of liquid and solid samples of functional materials and catalysts in the range of elements from F (№9) to transuranic elements (>№103). The range of determined concentrations from ppm to 100 % allows one to quickly and efficiently perform the analysis of solid, liquid or dispersed samples

### Equipment

#### X-ray fluorescence spectrometer ARL Perform'X (Thermo Scientific)

- Highly efficient tube 4GN with Rh anode and thin mechanical Be window (75 microns)
- Microprocessor-controlled universal goniometer without gears
- 7 flat crystals:

crystal	2d spacings
1 LiF200	4.0267
2 PET	8.7518
3 Ax06	57.8000
4 LiF220	2.8480
5 Ge111	6.5320
6 AXBeB	165.0000
7 AX16c	170.4000

- 4 primary collimators: 0.25°, 2.60°, 0.60°, 0.15°
- 2 detectors: scintillation and flow proportional
- The maximum angular velocity of 4800° 2 $\theta$ /min
- Angular accuracy on LiF crystals: +0,015°
- Angular reproducibility: <+0.0002°
- The total angular range: from 0° - 153° 2 $\theta$  (flow-proportional counter: 17° - 153°, scintillation counter: from 0° - 115°)
- Continuous digital scanning: from 0.25°/min to 327°/min depending on the time and measurement step

- Range scan step: tick:  $0.001^\circ$ . Maximum practical:  $1.00^\circ$ . Time of measurement for each step: from 0.1 to 655 seconds
- Multi-channel analyzer for the separation of high-energy peaks. Digital Automatic Gain Control (AGC) for the correction of pulse compression. Automatic dead time correction ensures linearity of response up to 2 M pulses per second on flow-proportional and 1.5 M pulses on a scintillation counter
- Basic Sample changer: 16 cassettes
- Cassettes for samples. Maximum size of sample: height 30 mm, diameter 52 mm. The hole diameter of 29 mm. Rotation of cassettes: 30 rpm
- Programmable 3-position filter of the primary radiation to optimize the X-ray excitation, Cu 0.25 mm: analysis of Ru, Rh, Pd, Ag and Cd (elements that are interfered by Rh line X-ray tube) and light variable matrices; Al 0.5 mm to improve peak to background ratio on Pb or As in light matrices; dust filter Be 0.127 mm
- Solid-state high-frequency X-ray generator with capacity of 3.6 kW, maximum voltage 60 kV and maximum current of 100 mA. Any combination of voltage kV and mA current should not exceed 3.6 kW



# Elemental Analysis

## Inductive-Coupled Plasma Mass-Spectrometry (ICP-MS)

### Scientific and analytical tasks

Investigation of elemental composition (in the range from Li to U) of liquid samples and solid samples which can be dissolved. This includes analysis of catalysts, functional materials and reaction mixtures as well as the initial components and reaction products

### Equipment

#### Agilent 7700 ICP-MS System

- **Low-flow nebulizer and Peltier-cooled Scott spray chamber**
  - The nebulizer and spray chamber and quartz, injection system for samples with a high content of matrix (HMI)
  - One-piece quartz torch with wide diameter (2.5 mm) injector
  - 3-channel, 10-roller peristaltic pump
- **Interface**
  - Ni interface cones
  - Dual on-axis extraction lenses
- **Vacuum System**
  - Single, 2-stage turbomolecular pump
  - Floor-mounted rotary pump
- **Gas Flow Control:** controls plasma, auxiliary, makeup, and carrier gas and Octopole Reaction System (ORS) reaction gas lines
- **Plasma and Ion Optics**
  - Plasma stabilization system
  - Torch xyz Position system
  - Solid state, digitally-driven 27 MHz RF generator
  - Off-axis Omega lens
  - Octopole reaction system
- **Mass-analyzer:** mass range 2 - 260 AMU, RF frequency: 3 MHz, minimum dwell time 100  $\mu$ s, abundance sensitivity  $< 5 \times 10^{-7}$  for low mass, for high mass  $< 1 \times 10^{-7}$
- **Dual-Mode Detection System**
  - Dual-mode discrete dynode detector with nine orders of linear dynamic range
  - Log amplifier circuit with a high-speed analog mode for transient signals (nine orders dynamic range)
- **Water cooler** (input pressure 230 - 400 KPa, min flow rate 15 l/min, input temperature 15 - 40 °C)

Agilent 7700 ICP-MS System



# Elemental Analysis

## Inductively Coupled Plasma Optical Emission Spectroscopy (ICP-OES)

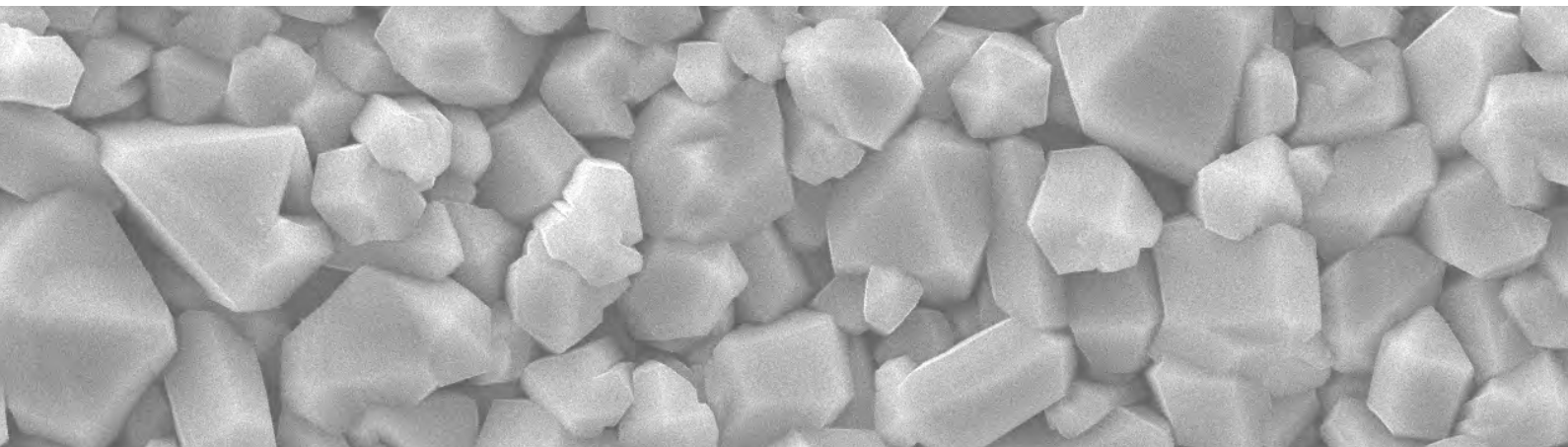
### Scientific and analytical tasks

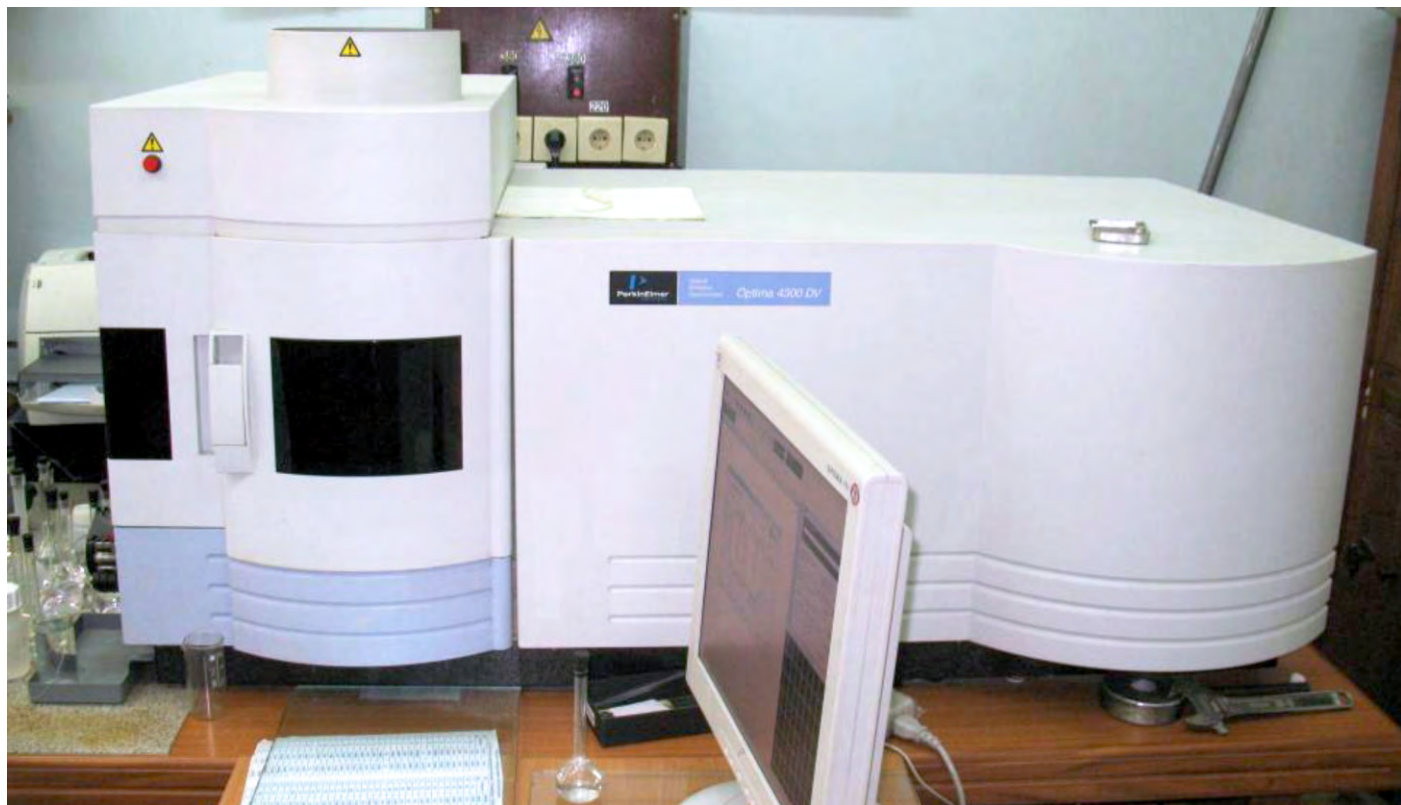
- Qualitative and quantitative analysis of up to 70 elements in the concentrations of dry matter from tens % to 0.0001 %. The analysis is performed from a solution
- Determination of the phase composition of solids by differential dissolution method

### Equipment

#### ICP-Optical emission spectrometer OPTIMA 4300 DV PerkinElmer

- The wavelength range: 180 - 800 nm
- Resolution of the spectrometer: 0.006 nm at 200 nm
- 40-MHz, free-running solid state (no power amplifier tube needed) RF generator, adjustable from 750 to 1500 watts, in 1 watt increments
- The system can routinely handle 50 % (w/v) solutions of HCl, HNO<sub>3</sub>, H<sub>2</sub>SO<sub>4</sub>, H<sub>3</sub>PO<sub>4</sub>, 20 % (v/v) HF and 30 % (w/v) NaOH
- A three-channel, computer-controlled pump with speed variable from 0.2 to 5 mL/minute in 0.1-mL/min increments using 0.76 mm (0.030") i.d. tubing
- The computer-controlled, pneumatically operated shutter automatically opens and closes for each sample
- Simultaneous determination of several elements in 1 - 2 min





ICP-Optical emission spectrometer  
OPTIMA 4300 DV PerkinElmer

## References

1. Determination of the phase composition of the intermediate and final products of the synthesis of Cu-Al cermets by a differential dissolution stoichiographic method.  
*Inorg. Mater.* **52** (2016) 331
2. determination of the phase composition of amorphous and crystalline copper ferrite-chromite samples by a reference-free method of differentiating dissolution.  
*J. Anal. Chem.* **70** (2015) 1229
3. Detecting spatial inhomogeneity manifestations in the chemical composition of functional materials by stoichiographic methods.  
*J. Struct. Chem.* **55** (2014) 1160
4. Determination of the phase composition of catalyst precursors for multiwall carbon nanotubes by the stoichiographic differential dissolution method.  
*J. Struct. Chem.* **55** (2014) 1166
5. Origin of the solid solution in the  $\text{LiInSe}_2\text{-In}_2\text{Se}_3$  system.  
*J. Solid State Chem.* **220** (2014) 91
6. Determination of the chemical composition of modified fiber glass silicate materials by differential dissolution.  
*J. Anal. Chem.* **68** (2013) 72
7. Determination of the chemical composition of supported vanadium-containing oxide catalysts by the differential dissolution method.  
*J. Anal. Chem.* **66** (2011) 88

# Chromatography

## Gas Chromatography (GC) Systems (>300 units)

### Scientific and analytical tasks

- Separation of the complex mixtures of low weight substances on capillary columns
- Capillary columns testing
- Multicapillary columns testing
- Separation of the complex mixtures by comprehensive two-dimensional chromatography
- Quality and quantity analysis of different substances

### Equipment

**Agilent 7890A Gas Chromatographic System with a flame ionization detector, Agilent G4513A autosampler and flow modulator for comprehensive two-dimensional chromatography**

#### **Column Oven:**

Sets the temperature: 25 - 380 °C

Temperature program speed: 0.1 - 48 C/min

**Injector:** Split/splitless mode

Injector temperature: 30 - 400 °C

**Detector:** FID

#### ***Comprehensive two-dimensional GC***

**Modulator:** flow-type

Modulation period: 1 - 10 s

**First column:** capillary

1<sup>st</sup> column carrier gas flow: 0.7 - 1.0 ml/min

**Second column:** capillary or multicapillary

2<sup>nd</sup> column carrier gas flow: 15 - 60 ml/min

Data frequency: up to 200 Hz



## References

1. Gas chromatography of the future: Columns whose time has come.  
*Russ. Chem. Rev.* **85** (2016) 1033
2. Separation of phenol-containing pyrolysis products using comprehensive two-dimensional chromatography with columns based on pyridinium ionic liquids.  
*J. Sep. Sci.* **39** (2016) 3754
3. The use of high-speed multicapillary column in comprehensive two-dimensional gas chromatography with flow modulation.  
*J. Chromatogr. A* **1426** (2015) 183
4. Thermostable columns based on ionic liquids for the analysis of hydrocarbon mixtures by two-dimensional chromatography.  
*Protection Metals Phys. Chem. Surfaces* **51** (2015) 1080
5. Stationary phases deposition on the planar columns capillaries.  
*Protection Metals Phys. Chem. Surfaces* **51** (2015) 1065
6. The properties of capillary columns with silica organic-inorganic MCM-41 type porous layer stationary phase.  
*J. Chromatogr. A* **1351** (2014) 103
7. Programming of temperature and flow rate of carrier gas in work with polycapillary columns for gas-liquid chromatography.  
*J. Anal. Chem.* **69** (2014) 559
8. The use of triazine polymer as a structured sorbent for chromatography.  
*Dokl. Phys. Chem.* **449** (2013) 75
9. Mass spectral evaluation of column bleeding for imidazolium-based ionic liquids as GC liquid phases  
*Anal. Bioanal. Chem.* **403** (2012) 2673
10. Single cation ionic liquids as high polarity thermostable stationary liquid phases for capillary chromatography.  
*Russ. J. Phys. Chem. A* **86** (2012) 138
11. Multicapillary columns with a porous layer based on the divinylbenzene copolymer.  
*Russ. J. Phys. Chem. A* **84** (2010) 871
12. Investigation of the loading capacity of multicapillary chromatographic columns.  
*J. Anal. Chem.* **65** (2010) 1129
13. Investigation of structure and properties of divinylbenzene-styrene copolymer films.  
*J. Struct. Chem.* **51** (2010) 164
14. Express gas chromatography on multicapillary columns and its potential.  
*Catal. Ind.* **2** (2010) 206
15. Sol-gel multicapillary columns for gas-solid chromatography.  
*J. Chromatogr. A* **1101** (2006) 315

## Gas Chromatography - Mass-Spectrometry (GC-MS) System

### Scientific and analytical tasks

- Component identification in complex mixtures of organic compounds
- Qualitative and quantitative analysis of the various classes of chemical compounds
- Determination of trace impurities in mixtures

### Equipment

#### Agilent 7000B Triple Quadrupole GC/MS/MS System with Agilent 7890A Gas Chromatograph

- Mode: electron impact
- Ion source temperature: 100 to 350 °C
- Electron energy: 10 to 300 eV
- Mass range: 10 - 1050 m/e



- Mass axis stability:  $\pm 0.10$  u over 24 hours (10 to 40 °C)
- Quadrupole temperature: 106 - 200 °C
- Resolution selectable: 0.7 to 2.5 Daltons, default tune
- Scan rate: up to 6.250 u/sec
- Tuning: autotune or manual
- MRM speed: 800 transition/sec
- Minimum MRM dwell: 0.5 msec
- Collision cell: linear hexapole
- Collision cell gas: nitrogen with helium quench gas
- Collision energy selectable: up to 60 eV
- Vacuum system: dual-stage turbomolecular pump
- Software: Agilent MassHunter

## References

1. Separation of phenol-containing pyrolysis products using comprehensive two-dimensional chromatography with columns based on pyridinium ionic liquids.  
*J. Sep. Sci.* **39** (2016) 3754
2. Thermostable columns based on ionic liquids for the analysis of hydrocarbon mixtures by two-dimensional chromatography.  
*Protection of Metals and Physical Chemistry of Surfaces* **51** (2015) 1080
3. Selectivity of stationary phases based on pyridinium ionic liquids for capillary gas chromatography.  
*Russ. J. Phys. Chem. A* **88** (2014) 717
4. Mass spectral evaluation of column bleeding for imidazolium-based ionic liquids as GC liquid phases.  
*Anal. Bioanal. Chem.* **403** (2012) 2673
5. Single cation ionic liquids as high polarity thermostable stationary liquid phases for capillary chromatography.  
*Russ. J. Phys. Chem. A* **86** (2012) 138

## High Performance Liquid Chromatography (HPLC)

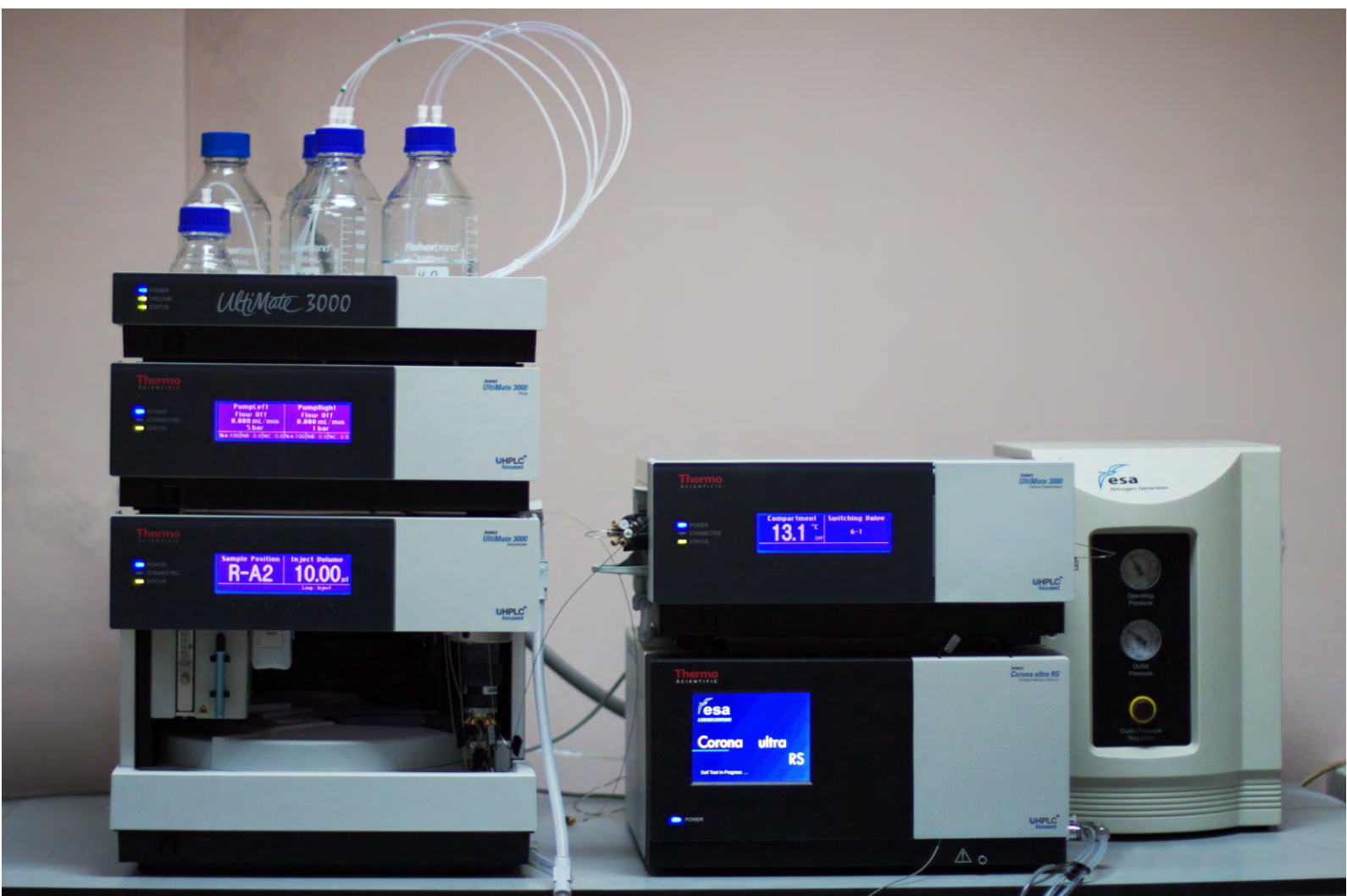
### Scientific and analytical tasks

- Separation of complex mixtures of small and macromolecules on the semimicropacked and monolithic columns
- Monolithic columns testing
- Quality and quantity analysis of different substances

## Equipment

### UltiMate 3000 UHPLC system (Thermo Scientific, USA)

- **Detector:** Corona Ultra charged aerosol detector (CAD)
- **Pump:** Dual ternary gradient pump DGP-3600SD
- **Autosampler:** Integrated autosampler WPS-3000SL
- **Column:** Compatibility with any of columns,  
operating at pressures: up to 620 bar
- **Column Oven:** Sets the temperature 5 °C above ambient - 80 °C



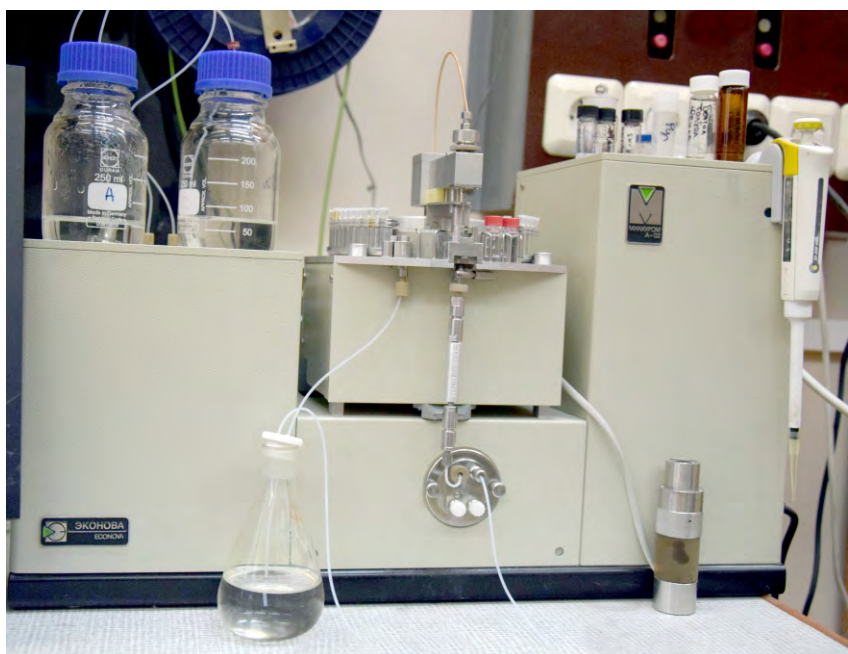
## Varian ProStar 500 Series liquid chromatograph (Varian B.V., USA)

- **Detector:** Refractometric detector (ProStar 355 RI Detector), UV detector
- **Column:** 250 × 4,6mm ×1,4" PetroSpher 5 A, B
- **Column Oven:** Sets the temperature 40 °C



## Milichrom A-02 HPLC microcolumn chromatograph (Econova, Russia)

- **Detector:** double-beam, multiwavelength UV-spectrophotometer  
Wavelength range: 190 - 360 nm  
Supporting up to 1 - 8 simultaneous wavelengths  
Flow cell volume: 1.2 µl
- **Pump:** double syringe  
Volume: 2 × 2500 µl
- **Autosampler:** programmable  
Number of samples: 46  
Sample volume: 1 - 99 µl
- **Column Oven:**  
Sets the temperature 35 - 90 °C



The logo for Thermo Scientific, with 'Thermo' in red and 'SCIENTIFIC' in black below it.A control panel with three indicator lights: a blue light labeled 'POWER', a yellow light labeled 'CONNECTED', and another yellow light labeled 'STATUS'. A large blue light is visible on the right side of the panel.

## References

1. Levopimaric acid derived 1,2-diamines and their application in the copper-catalyzed asymmetric Henry reaction. *Tetrahedron Lett.* **74** (2018) 260
2. Iminodiacetic acid synthesis over Cu/ZrO<sub>2</sub> catalyst in a microchannel flow reactor. *Chemical Engineering J.* **330** (2017) 899
3. Hydroprocessing of straight run diesel mixed with light cycle oil from fluid catalytic cracking, using sulfide NiMo catalyst on zeolite-containing supports. *Catal. Industry* **9** (2017) 212
4. N-phosphonomethyl iminodiacetic acid N-oxide synthesis in the presence of bifunctional catalysts based on tungsten complexes. *Catal. Com.* **71** (2015) 102
5. Triethanolamine synthesis in a continuous flow microchannel reactor. *Chem. Eng. J.* **259** (2015) 252
6. Catalytic properties of CoMo/Al<sub>2</sub>O<sub>3</sub> sulfide catalysts in the hydrotreating of straight-run diesel fraction mixed with rapeseed oil. *Kinet. Catal.* **55** (2014) 481
7. The ionic liquid [bmim]Br as an alternative medium for the catalytic cleavage of aromatic C-F and C-Cl bonds. *Tetrahedron Lett.* **51** (2010) 2265
8. Modern catalysts of deep hydrotreatment in the production of low-sulfur diesel fuels at Russian oil refineries according to Euro-3 and Euro-4 standards. *Catal. Industry* **2** (2010) 101
9. Bimetallic Co-Mo complexes: A starting material for high active hydrodesulfurization catalysts. *Catal. Today* **150** (2010) 196
10. Activity and sulfidation behavior of the CoMo/Al<sub>2</sub>O<sub>3</sub> hydrotreating catalyst: The effect of drying conditions. *Catal. Today* **149** (2010) 19
11. Co-Mo catalysts for ultra-deep HDS of diesel fuels prepared via synthesis of bimetallic surface compounds. *J. Mol. Catal. A: Chem.* **322** (2010) 80
12. The superior activity of the CoMo hydrotreating catalysts, prepared using citric acid: What's the reason? *Studies in Surface Science and Catalysis* **175** (2010) 109
13. EXAFS study of oxide precursors of the high active Co-Mo hydrotreating catalysts: Effect of drying conditions. *Nuclear Instruments and Methods in Physics Research Section A* **603** (2009) 119
14. Reaction of pentafluoroacetanilide with zinc catalyzed by nickel complexes. *Russian Chemical Bulletin International Edition* **58** (2009) 2304

# Textural Methods of Investigation

## Static Vacuum Volumetry, Gas Adsorption, Low Temperature Gas Adsorption

### Scientific and analytical tasks

- Studies of texture of catalysts and adsorbents
- Measurements of surface area, pore volume and pore size distribution

### Equipment

- **Autosorb-iQ2-MP/AG (Quantachrome Instruments, USA)**

#### Features

- Fully automatic analysis of surface area, pore volume and pore size
- High-resolution isotherm for accurate refinement of pore structure
- High performance and analysis flexibility with dedicated P and analysis stations:
  - Micropore analysis station with  $P/P 10^{-7} - 0.9995$
  - Mesopore analysis station with  $P/P 10^{-3} - 0.9995$
- Various dosing methods for best accuracy and performance

#### Specifications

- Surface area range: from  $0.01 \text{ m}^2/\text{g}$  to no known upper limit (nitrogen)
- Low limit of pore volume (liquid volume):  $1 \times 10^{-6} \text{ ml/g}$
- Pore size range: 0.35 - 500 nm
- Coolant dewar: 1 (3L), up to 100 hours of unattended operation

#### Pressure transducers specifications

- Upper pressure limits: 1000, 10 and 1 Torr
- Pressure resolution (1 Torr): 0.00000026 Torr
- Accuracy (1000 Torr): 0.11 % (full range)
- Accuracy (10 and 1 Torr): 0.15 % of readings

- **Quadrasorb evo (Quantachrome Instruments, USA)**

#### Features

- Fully automatic analysis of surface area, pore volume and pore size. High-resolution isotherm for accurate refinement of pore structure
- High performance and analysis flexibility with dedicated  $P^\circ$  and analysis stations (4 stations with  $P/P^\circ 10^{-3} - 0.9995$ )
- Various dosing methods for best accuracy and performance

## Specifications

- Surface area range: from 0.01 m<sup>2</sup>/g to unknown upper limit (nitrogen)
- Low limit of pore volume (liquid volume): 1 × 10<sup>6</sup> ml/g
- Pore size range: 0.35 - 500 nm
- Coolant dewars: 4 (2L), up to 30 hours of unattended operation

## Pressure transducers specifications

- Upper pressure limits: 1000 Torr
- Pressure resolution: 0.00026 Torr
- Accuracy: 0.11 % (full range)

## • Autosorb-6B-Kr (Quantachrome Instruments, USA)

### Features

- Fully automatic analysis of surface area, pore volume and pore size
- High-resolution isotherm for accurate refinement of pore structure
- High performance and analysis flexibility with dedicated P and analysis stations: six stations equipped with 1000 Torr transducers and one 1 Torr transducer onto manifold

### Specifications

- Surface area range: from 0.1 m<sup>2</sup>/g to no known upper limit (nitrogen)
- Low limit of pore volume (liquid volume): 1 × 10<sup>4</sup> ml/g
- Pore size range: 0.35 - 400 nm
- Coolant dewar: 1 (2.5 L), up to 35 hours of unattended operation

### Pressure transducers specifications

- Upper pressure limits: 1000 and 10 Torr
- Pressure resolution (10 Torr): 0.0000026 Torr
- Accuracy (1000 Torr): 0.11 % (full range)
- Accuracy (10 Torr): 0.15 % of readings
- Accuracy (1000 Torr): 0.1 % (full range)



Autosorb-iQ2-MP/AG, Quadrasorb evo



Autosorb-6B-Kr



ASAP-2400

- **ASAP-2400 (Micromeritics Corp., USA)**

### Features

- Fully automatic analysis of surface area, pore volume and pore size
- High performance and analysis flexibility with dedicated P and six analysis stations: six stations equipped with 1000 Torr transducers

### Specifications

- Surface area range: from 1 m<sup>2</sup>/g to no known upper limit (nitrogen)
- Low limit of pore volume (liquid volume): 1 × 10<sup>-3</sup> ml/g
- Pore size range: 0.35 - 200 nm
- Coolant dewar: 6 (2 L), up to 24 hours of unattended operation

### Pressure transducers specifications

- Upper pressure limits: 1000 Torr
- Accuracy (1000 Torr): 0.1 % (full range)

## References

1. Method for evaluation of BET adsorbed monolayer capacity. *Microporous and Mesoporous Mater.* **243** (2017) 147
2. Fe-silicalites as heterogeneous Fenton-type catalysts for radiocobalt removal from EDTA chelates. *Appl. Catal., B* **185** (2016) 353
3. One-step solvent-free synthesis of cyclic carbonates by oxidative carboxylation of styrenes over a recyclable Ti-containing catalyst. *Appl. Catal., B* **181** (2016) 363
4. CoMoNi catalyst texture and surface properties in heavy oil processing. Part I: Hierarchical macro/mesoporous alumina support. *Industrial & Engineering Chem. Res.* **55** (2016) 3535
5. Mesoporous Fe-alumina films prepared via sol-gel route. *Microporous and Mesoporous Mater.* **204** (2015) 276
6. Micro-mesoporous carbons from rice husk as active materials for supercapacitors. *Materials for Renewable and Sustainable Energy* **4** (2015) 20
7. Highly selective H<sub>2</sub>O<sub>2</sub>-based oxidation of alkylphenols to p-benzoquinones over MIL-125 metal-organic frameworks. *Eur. J. Inorg. Chem.* **1** (2014) 132
8. User-friendly synthesis of highly selective and recyclable mesoporous titanium-silicate catalysts for the clean production of substituted p-benzoquinones. *Catalysis Science & Technology* **4** (2014) 200
9. Effect of iron content on selectivity in isomerization of α-pinene oxide to campholenic aldehyde over Fe-MMM-2 and Fe-VSB-5. *Appl. Catal., A* **469** (2014) 427
10. Environmentally benign oxidation of alkylphenols to p-benzoquinones: A comparative study of various Ti-containing catalysts. *Top. Catal.* **57** (2014) 1377
11. Meso/macroporous CoMo alumina pellets for hydrotreating of heavy oil. *Industrial & Engineering Chemistry Research* **52** (2013) 17117
12. A study of microporous aluminophosphates obtained in the presence of symmetrical di-n-alkylamines. *Russ. Chem. Bull.* **61** (2012) 1867

## Mercury Porosimetry

### Scientific and analytical tasks

- Characterization of material's porosity by applying various levels of pressure to a sample immersed in mercury. The pressure required to intrude mercury into the sample's pores is inversely proportional to the size of the pores
- Mercury porosimetry is used as an analytical technique for studies of porous structure of solid catalysts, adsorbents, rocks and other materials. The range of pore sizes: 3 nm - 1 mm, the range of pore volumes: 0.05 - 0.30 cc/g with a step of 0.001 cc

### Equipment

- Measuring pore diameters from 0.003 to 1000  $\mu\text{m}$
- Low noise, high-pressure generating system
- Enhanced data reduction package; includes calculation of tortuosity, permeability, compressibility, pore-throat ratio, fractal dimension, Mayer-Stowe particle size, and more
- Operates in scanning and time/rate equilibrated modes
- Collects extremely high-resolution data; better than 0.1  $\mu\text{L}$  for mercury intrusion and extrusion volumes
- Controlled evacuation prevents powder fluctuation



## Chemical Adsorption and Temperature-Programmed Reactions

### Scientific and analytical tasks

- Qualitative estimates of metal dispersion and active area in supported catalysts with Group VIII elements [1-4] and Ag [5]
- Studies of the state of supported nanoparticles and sub-nanoclusters, the metal-support interaction, and structural changes under the influence of adsorbate [1]

## Equipment

### Chemisorption Analyzer AutoChem II 2920 (Micromeritics)

- The instrument performs pulse chemisorption, temperature-programmed desorption, reduction, and oxidation (TPD, TPR, TPO) automatically
- Three independent gas lines with twelve gas inlets provide the capability to perform *in situ* pretreatments and sequential experiments with the same sample in different gas media
- The internal temperature-controlled zones can be heated independently up to 150 °C, which prevents any condensation in the flow path
- Four high-precision, independently calibrated mass flow controllers provide extremely accurate, programmable gas control (in the range of 1 - 100 ml/min)
- The instrument is provided with highly sensitive linear thermal conductivity detector (TCD) which assures the calibration volume remains constant over the full range of peak amplitudes
- Clamshell furnace can heat the quartz sample reactor to 1100 °C at a constant ramp rate (1 - 50 K/min)

### References

1. Probing the H<sub>2</sub>-induced restructuring of Pt nanoclusters by H<sub>2</sub>-TPD. *Langmuir* **32** (2016) 12013
2. Single atoms of Pt-group metals stabilized by N-doped carbon nanofibers for efficient hydrogen production from formic acid. *ACS Catalysis* **6** (2016) 3442
3. Synthesis of Pt/C catalysts through reductive deposition: Ways of tuning catalytic properties. *Chem. Cat. Chem.* **5** (2013) 2015
4. Preparation of platinum-on-carbon catalysts via hydrolytic deposition: Factors influencing the deposition and catalytic properties. *Appl. Catal. A: Gen.* **449** (2012) 203
5. High activity in CO oxidation of Ag nanoparticles supported on fumed silica. *Catal. Commun.* **22** (2012) 43



## Temperature-Programmed Methods (Reduction, Oxidation, Desorption), TPX (X=R, O, D, SR)

### Scientific and analytical tasks

- Chemisorption/physisorption for B.E.T. surface area and pore volume
- Determination of relative acid strengths
- Calculation of activation energies for a given reaction
- Quick screening of experimental catalysts, evaluation of efficiency of regeneration of used catalysts, determination of optimal catalyst preparation conditions for industrial use

### Equipment

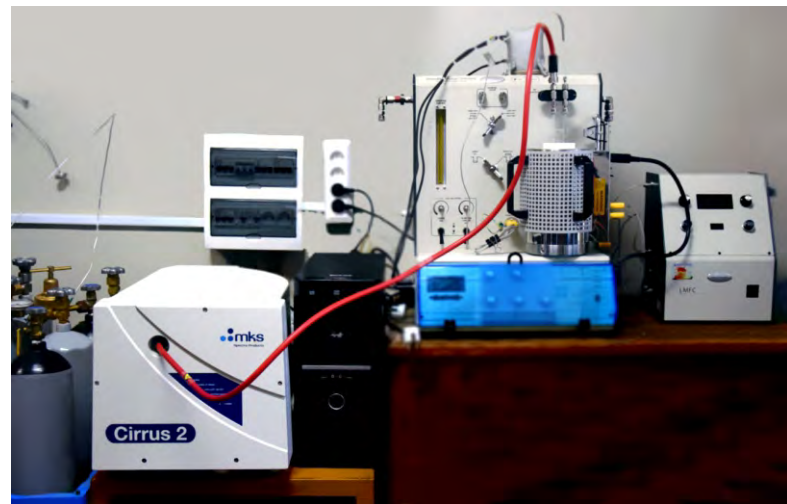
#### Automatic Chemisorption Analyzer ChemBET Pulsar TPR/TPD (Quantachrome, USA) with Cirrus-2 quadrupole mass-spectrometer (MKS, USA)

- **ChemBET:**

- Two-station set up (Outgas/preparation station + analysis station)
- 3 exchangeable injection loops with volume of 0.05, 0.1 and 0.25 mL
- Quartz glassware with self-sealing cell holders
- In line cold trap with bypass line
- 5 gas input ports + gas mixer & linear mass flow controller
- High temperature heating mantle (450 °C) and furnace (1100 °C)
- Software controlled temperature ramping, °C/min: 100 / 50 / 30 / 20 within the ranges of 500 °C / 750 °C / 1000 °C / 1100 °C
- Surface area range: 0.1 - 280 m<sup>2</sup>
- Pore volume range: 0.0001 - 0.15 mL
- Reproducibility: 0.5 %
- Chemically resistant set up for analyzing:  
H<sub>2</sub>, O<sub>2</sub>, CO, NO, SO<sub>2</sub>, NH<sub>3</sub> (chemisorption)  
N<sub>2</sub>, Ar, Kr, CO<sub>2</sub> +He (physical adsorption)

- **Corrosion resistant thermal conductivity detector Cirrus-2:**

- 200 amu mass range
- Dual Faraday Cup/SEM detector
- Tungsten cathode
- Heated fused silica capillary inlet
- Nominally atmospheric pressure
- Pumping stand equipped with turbomolecular pump



# Steady-State Isotopic Transient Kinetic Analysis (SSITKA)

## Determination of Kinetics and Catalyst Surface Reaction Intermediates *In Situ*

### Scientific and analytical tasks

- Study of ionic mobility and surface reactivity of materials
- Study of gas-phase and vapour-phase catalytic reactions mechanisms

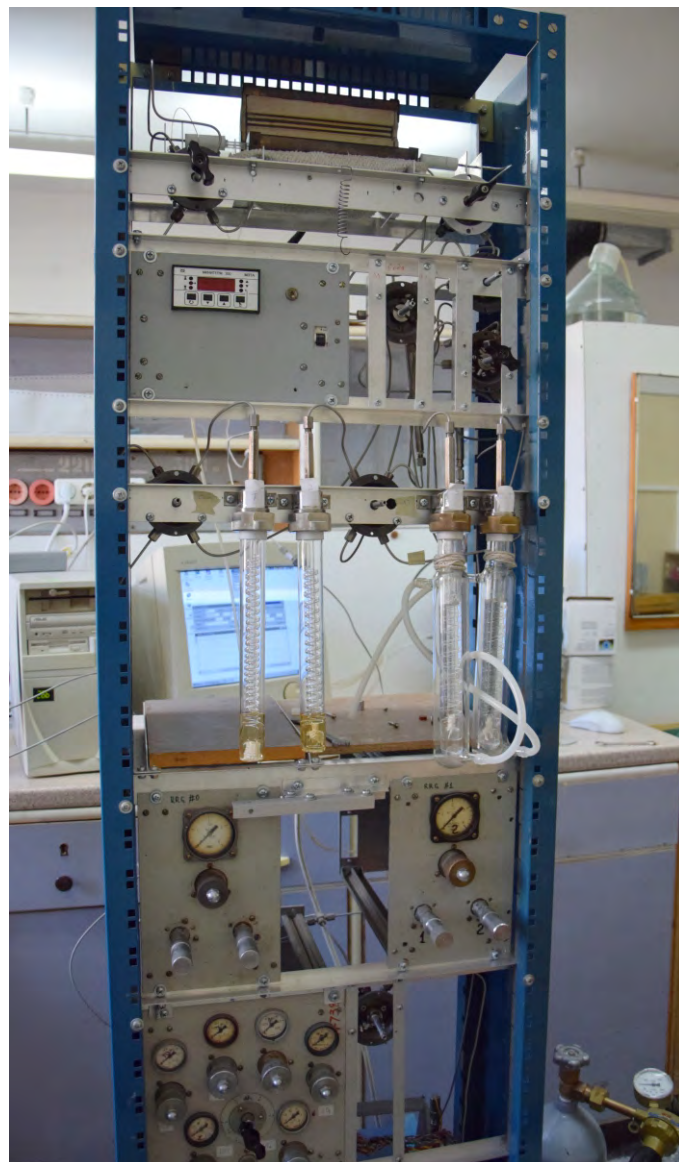
### Equipment

#### Setup with a fixed-bed reactor

- **Flow Mass Controller (Kvarta, Novosibirsk)** with **ChemLab 3** software
- Tube furnace equipped with **Miniterm PID controller** allowing to work in isothermal and programmed mode at temperature up to 800 °C
- **UGA-200 mass-spectrometer** (Stanford Research Systems, USA) with **UGA3** and **RGA3** software

#### Specifications:

<http://www.thinksrs.com/downloads/PDFs/Manuals/UGAm.pdf>



## References

1. Structural studies of Pr nickelate-cobaltite - Y-doped ceria nanocomposite.  
*J. Ceramic Sci. Technol.* (2017) DOI: 10.4416/JCST2016-00099.
2. Temperature-programmed C<sup>18</sup>O<sub>2</sub> SSITKA for powders of fast oxide-ion conductors: Estimation of oxygen self-diffusion coefficients.  
*Solid State Ionics* **271** (2016) 69
3. Oxygen mobility in microwave sintered praseodymium nickelates-cobaltites and their nanocomposites with yttria-doped ceria.  
*Solid State Ionics* **288** (2016) 76
4. Structural and transport properties of doped LAMOX - electrolytes for IT SOFC.  
*Solid State Ionics* **288** (2016) 103
5. Sm-doped praseodymium nickelates-cobaltites and their nanocomposites with Y-doped ceria as promising cathode materials.  
*Integrated Ferroelectrics* **173** (2016) 71
6. Application of SR methods for the study of nanocomposite materials for hydrogen energy.  
*Physics Procedia* **84** (2016) 397
7. The conductivity and ionic transport of doped bismuth titanate pyrochlore Bi<sub>1.6</sub>M<sub>x</sub>Ti<sub>2</sub>O<sub>7-6</sub> (M - Mg, Sc, Cu).  
*Solid State Ionics* (2016) DOI: 10.1016/j.ssi.2016.12.019.
8. Methods of isotopic relaxations for estimation of oxygen diffusion coefficients in solid electrolytes and materials with mixed ionic-electronic conductivity.  
*Russ. J. Electrochem.* **51** (2015) 458
9. Oxygen mobility and surface reactivity of PrNi<sub>1-x</sub>Co<sub>x</sub>O<sub>3-δ</sub> perovskites and their nanocomposites with Ce<sub>0.9</sub>Y<sub>0.1</sub>O<sub>2-δ</sub> by temperature-programmed isotope exchange experiments.  
*Solid State Ionics* **273** (2015) 35
10. Solid oxide fuel cell cathodes: Importance of chemical composition and morphology.  
*Catal. Sustainable Energy* **2** (2015) 57
11. Oxygen mobility and surface reactivity of PrNi<sub>1-x</sub>Co<sub>x</sub>O<sub>3-δ</sub>-Ce<sub>0.9</sub>Y<sub>0.1</sub>O<sub>2-δ</sub> cathode nanocomposites.  
*Solid State Ionics* **262** (2014) 707
12. Cathodic materials for intermediate-temperature solid oxide fuel cells based on praseodymium nickelates-cobaltites.  
*Russ. J. Electrochem.* **50** (2014) 669
13. IT SOFC cathodes based on Pr nickelates/cobaltites: Design and performance.  
*Proceedings of the 11th European SOFC and SOE Forum, 1 - 4 July 2014, Lucerne/Switzerland, Chapter. 2014. - T.10. - P. 20-28.*
14. Fast oxygen transport in bismuth oxide containing nanocomposites.  
*Solid State Ionics* **251** (2013) 34
15. Mechanism of oxygen transfer in layered lanthanide nickelates Ln<sub>2</sub>NiO<sub>4+δ</sub> (Ln = La, Pr) and their nanocomposites with Ce<sub>0.9</sub>Gd<sub>0.1</sub>O<sub>2-δ</sub> and Y<sub>2</sub>(Ti<sub>0.8</sub>Zr<sub>0.2</sub>)<sub>1.6</sub>Mn<sub>0.4</sub>O<sub>7-δ</sub> solid electrolytes.  
*Russ. J. Electrochem.* **49** (2013) 645

# Calorimetry

## Calorimetry. Thermal Analysis

### Scientific and analytical tasks

Determination of thermal effects of adsorption, chemical reactions, and individual reaction stages

### Equipment

#### Differential Scanning Calorimeter Setaram SENSYS DSC TG

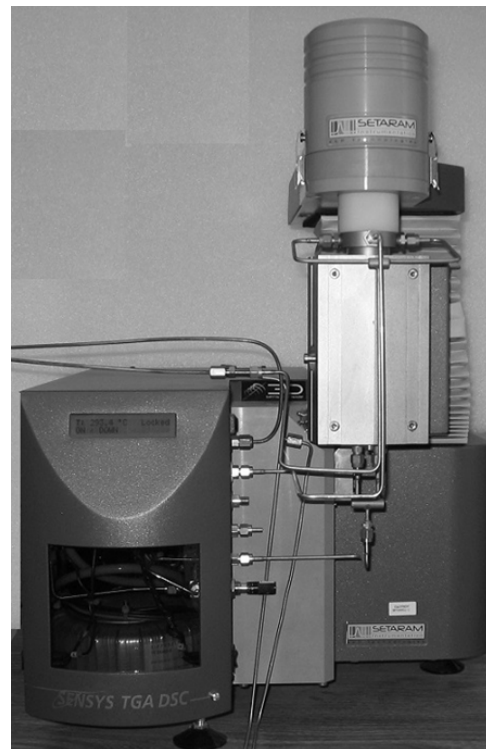
It includes calorimetric unit coupled with microbalance. It is possible to work in flow reactor mode in combination with chromatographic analysis.

- 3D Calvet sensor
- Temperature range: to 830 °C
- Programmable temperature scanning rate: 0.01 - 30 °C /min
- Crucibles: to 150  $\mu$ l
- TG Resolution: to 0.02  $\mu$ g

#### Pulse kinetic installation

Designed to supply gas-phase reagents in continuous or pulse mode

- Pulse volume 0.85 - 3.6 mL
- Up to six reagents can be plugged



### References

1. IR spectroscopic and calorimetric study of water and formic acid adsorption on a vanadium-titanium catalyst. *Kinet. Catal.* **56** (2015) 237
2. Mechanism of CH<sub>4</sub> dry reforming by pulse microcalorimetry: Metal nanoparticles on perovskite/fluorite supports with high oxygen mobility. *Thermochimica Acta* **567** (2013) 27
3. Ethanol selective oxidation into syngas over Pt-promoted fluorite-like oxide: SSITKA and pulse microcalorimetry study. *Catalysis Today* **278** (2016) 157

Polycrystalline platinum foil after ammonia oxidation by air in laboratory reactor at 1133 K during 1 hour



1 μm

## Remarks